



# Development of a rational design methodology for precast concrete slender spandrel beams: Part 2, analysis and design guidelines

Gregory Lucier,  
Catrina Walter, Sami Rizkalla,  
Paul Zia, and Gary Klein

## Editor's quick points

- This paper summarizes the results of an analytical research program undertaken to develop a rational design procedure for precast concrete slender spandrel beams.
- The analytical and rational models use test results and research findings of an extensive experimental program presented in a companion paper.
- The overall research effort demonstrated the validity of using open web reinforcement in precast concrete slender spandrel beams and proposed a simplified procedure for design.

Design and analysis of precast concrete slender spandrel beams is not a simple task because of eccentrically applied loads, lateral support conditions, and asymmetrical cross sections. Significant shear and torsion stresses develop in the end regions and act in combination with in-plane and out-of-plane bending stresses. When vertical eccentric loads are applied to the ledge or corbels of a typical slender spandrel beam, it will deflect downward, laterally inward at the top edge of the web, and laterally outward at the bottom edge of the web at midspan. The combination of vertical and lateral deflections results in a warped deflected shape and a tied arch cracking pattern. It is well documented that face-shell spalling and spiral cracking do not develop in slender spandrel beams at failure, though these limit-state behaviors are implicitly assumed in current practice.<sup>1-5</sup> The design method found in the sixth edition of the *PCI Design Handbook: Precast and Prestressed Concrete*<sup>6</sup> often results in conservative, heavy reinforcement

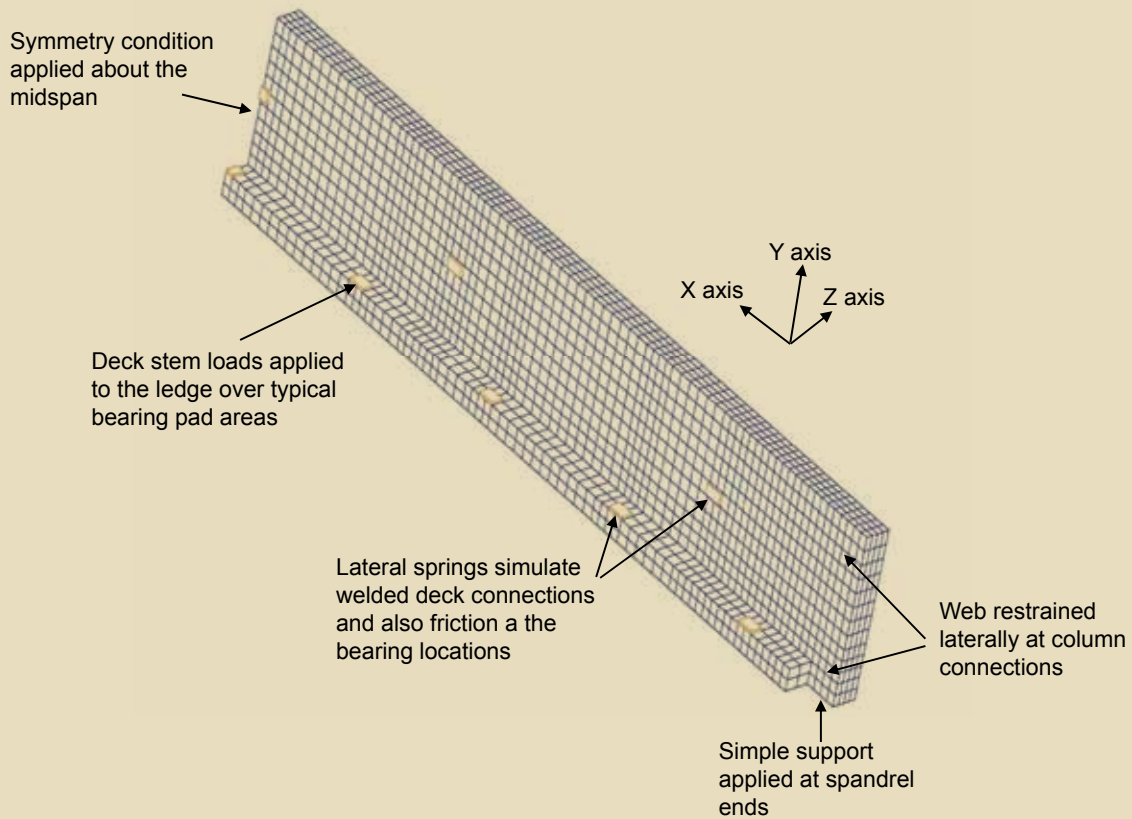


**Figure 1.** Typical mesh configuration for nonlinear finite element analytical model (L-shaped spandrel).

when used for slender spandrel beams, which often have aspect ratios much greater than 3.0.<sup>3,7</sup>

This paper discusses the design and analysis of precast concrete slender spandrel beams. The experimental program on which it is based was reported in the companion paper.<sup>1</sup>

## Objective

The objective of this research was to develop rational design guidelines for precast concrete slender spandrel beams with an aspect ratio (height divided by width) of at least 4.6. The guidelines are expected to simplify the reinforcement detailing required for slender spandrels, especially in the end regions. Specifically, the research focused on investigating whether traditional closed stirrups are required for the slender cross sections of typical precast concrete L- and corbelled spandrels. The use of open web reinforcement in lieu of closed stirrups would greatly simplify fabrication and reduce the cost of production.

## Nonlinear finite element analysis

A three-dimensional nonlinear finite element model (FEM) was developed and then calibrated with experimental

results<sup>1</sup> to study the various parameters that influence the behavior of slender L-shaped spandrel beams.

The finite element code ANACAP used in this study is capable of analyzing plain, reinforced, or prestressed concrete members in three dimensions. The program has extensive nonlinear capabilities and includes an advanced concrete material model. Additional details describing the finite element code can be found elsewhere.<sup>2</sup>

## Nonlinear finite element model

Considering symmetry, the nonlinear finite element analysis was based on modeling one-half of a typical slender spandrel beam using approximately 4,700 twenty-node brick elements. The exact number of elements varied depending on the specifics of the case under study. The large number of elements was necessary to maintain a sufficiently fine mesh around all of the loading and boundary conditions as well as in the end region, where failure was expected to occur. The modeled portion of a typical 45-ft-long (13.7 m) beam consisted of five ledge loads, three tieback connections, two lateral end restraints, one primary vertical end reaction, and a symmetry condition at midspan. **Figure 1** shows the finite element mesh and boundary conditions used for a typical L-shaped spandrel.



Several parameters were examined using the nonlinear FEM. These parameters included closed versus open web reinforcement, web reinforcement type and ratio, cross section dimensions, concrete strength, and the influence of boundary conditions such as bearing friction and deck connections.

## Boundary conditions

The boundary conditions used in the model were chosen to simulate the connections typically used to support spandrel beams in the field. The spandrel-to-column tiebacks were simulated by restraining lateral movement at those two locations in the model. Vertical movement was restrained in the bearing area of the main vertical reaction. Symmetry boundary conditions were applied at midspan. Each vertical load applied to the spandrel ledge was modeled as uniform pressure acting on an area equal to the size of the bearing pads used in the experimental program. These applied loads were increased incrementally until failure.

Spring elements were used to simulate stem-to-ledge bearing friction and deck-to-spandrel tieback forces. For the deck connections, the stiffness of the spring elements was estimated based on the material and cross-sectional properties of the weld plate. The spring constant simulating the friction at bearing reactions was determined based on the coefficient of friction for the chosen bearing pads. The coefficient of friction for a given bearing pad was assumed to remain constant at all levels of applied load. These assumptions tended to slightly overestimate the friction force at high overload levels when the out-of-plane behavior became significantly nonlinear.

Selected results from the nonlinear finite element analysis are presented in the following sections.

## Deflected shape and cracking pattern

**Figure 2** shows the predicted and observed inner web face cracking patterns in the end region of a reinforced concrete L-spandrel, a prestressed concrete L-spandrel, and a prestressed concrete corbelled spandrel. For clarity, the observed cracking patterns were photographed after failure with the deck sections removed. The analytical cracking patterns are shown at the factored load level for clarity. Only half of each beam is shown in the figure because the analysis was symmetric about the midspan.

In general, the predicted deformed shape was a combination of vertical and lateral deflections, and matched well to the observed behavior. The midspan of the beam moved downward, and the top of the web rolled inward toward the applied loads at midspan. The degree of lateral deformation was influenced by the deck connections, as discussed in detail in the technical report.<sup>2</sup>

**Figure 2** indicates that the predicted cracking patterns matched well with those observed in experiments. Flexural cracking was observed in the midspan region, primarily on the outer web face. A primary diagonal crack initiated in the end region at the face of the support. This crack extended upward at an angle of approximately 45 deg. Away from the end region, the crack angles began to flatten and arch toward midspan.

The predicted cracking pattern for a reinforced concrete L-spandrel shows extensive flexural cracking at midspan, as expected for a nonprestressed concrete beam. In comparison, analysis of a prestressed concrete L-spandrel showed little flexural cracking at corresponding load levels. These predictions were confirmed by observed cracking patterns. The primary diagonal crack developed from the face of the support for all three selected beams. One interesting difference is that the predicted angle of this crack is almost 45 deg for the reinforced concrete beam, and as expected, it was flatter for the two prestressed concrete beams closer to 35 deg. This finding was not confirmed by the tests, as shown in the photographs in the left column of **Fig. 2**. While cracks on the inner face of the prestressed concrete beams flattened out more rapidly than did cracks on comparable nonprestressed concrete beams, there was minimal difference in the angle of the primary crack extending from the support of each specimen.

## Failure mode

**Figure 3** shows the failure modes predicted by the nonlinear FEM for the same three selected beams alongside the observed failure modes. The failure mode determined from analysis is illustrated by plotting the predicted shearing strain contours in the plane of the web face. All beams in **Fig. 3** were reinforced with additional flexural and local reinforcement to avoid premature flexural failure and induce end-region behavior, as described in the companion paper.<sup>1</sup> The comparison shown in the figure indicates that the analytical model was capable of predicting the observed skewed-diagonal end-region failure mode for the L-shaped and corbelled spandrels.

## Deflections

**Figure 4** compares a representative vertical load-deflection prediction with the experimental results. The initial stiffness of the predicted load-deflection curves tended to be slightly higher than the measured values; however, the predicted stiffness tended to match closely to measured values after cracking. The analytical model closely predicted the failure load and failure deflection, with some deviation in the final stages of loading.

**Figure 5** shows the predicted and measured lateral deflections for a representative spandrel beam. The comparison highlights the effect of short-term creep during the test, as evidenced by horizontal portions of the load-deflection



	Experimental cracking	Analytical cracking
<b>Reinforced concrete</b> <b>L-spandrel</b> <b>SP10.8L60.45.R.O.E.</b>		
<b>Prestressed concrete</b> <b>L-spandrel</b> <b>SP12.8L60.45.P.O.E.</b>		
<b>Prestressed concrete</b> <b>corbelled spandrels</b> <b>SP17.8CB60.45.R.O.E.</b>		

**Figure 2.** Comparison of experimental cracking and analytical cracking. Note: the detailed specimen names are for reference to the companion paper.

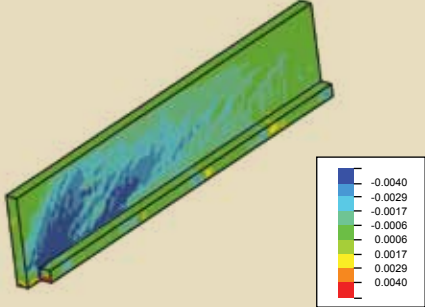
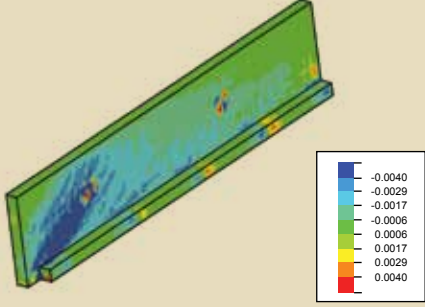
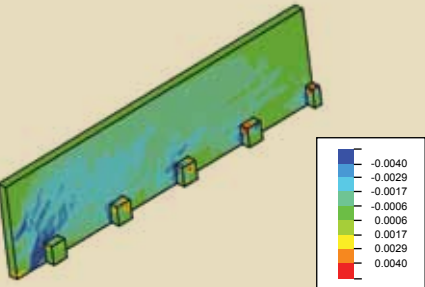
behavior. Short-term creep was especially prominent over the 24-hour sustained load tests. The FEMs do not account for creep. If creep effects were removed, representing an experimental test conducted without sustained loading, the experimental results would match the predicted values more closely. The predicted lateral deflections matched well the experimental values through most of the tested range. The FEM captured the spandrel behavior with the top edge of a slender spandrel beam moving inward and the bottom edge moving outward at midspan, pivoting about the deck connection. Further description of the finite element analysis is presented along with the full analytical results in the research report.<sup>2</sup>

### Rational model

Based on the observed behavior and the nonlinear finite element analysis, a rational model was developed to describe the behavior of a slender spandrel beam. The rational model forms the basis of the proposed simplified design approach, presented later in this paper. The model is based on equilibrium of forces at the diagonal skewed failure plane observed in the experimental program.

The design principles are only applicable for the modeling of slender beams with an aspect ratio equal to or greater than 4.6 as this was the smallest aspect ratio tested. The beams considered had the following controls:



	Experimental failure mode	Analytical failure mode
<b>Reinforced concrete</b> <b>L-spandrel</b> <b>SP10.8L60.45.R.O.E.</b>		 Contour Plot of Shearing Strains
<b>Prestressed concrete</b> <b>L-spandrel</b> <b>SP12.8L60.45.P.O.E.</b>		 Contour Plot of Shearing Strains
<b>Prestressed concrete</b> <b>corbelled spandrels</b> <b>SP17.8CB60.45.R.O.E.</b> <b>(photo mirrored)</b>	 (photo mirrored for consistency, actual failure was on right side)	 Contour Plot of Shearing Strains

**Figure 3.** Comparison of experimental failure modes with analytical failure modes.

- They were supported at each end by two horizontal reactions that form a couple to provide torsional stability.
- They were simply supported for gravity load.
- They had loads applied to a continuous ledge or to discrete corbels located along the bottom edge of one web face.
- They had a ledge or corbels designed according to the standard procedures recommended by the *PCI Design Handbook*.

Inspection of the cracking pattern of all tested slender

spandrel beams loaded to failure allowed for identification of the following three distinct zones (**Fig. 6**).

### End region

The end region is defined as the portion of the beam from the end to a distance  $h$  from the face of the support. The test results of full-sized spandrels reported in the companion paper<sup>1</sup> indicate that the angle of the critical diagonal crack that developed on the inner web face within this region is 45 deg. The observed failure mode clearly indicated that plate bending, vertical shear, and lateral shear (twist) dominate the end-region response because shear and torsion demands are highest in this region.

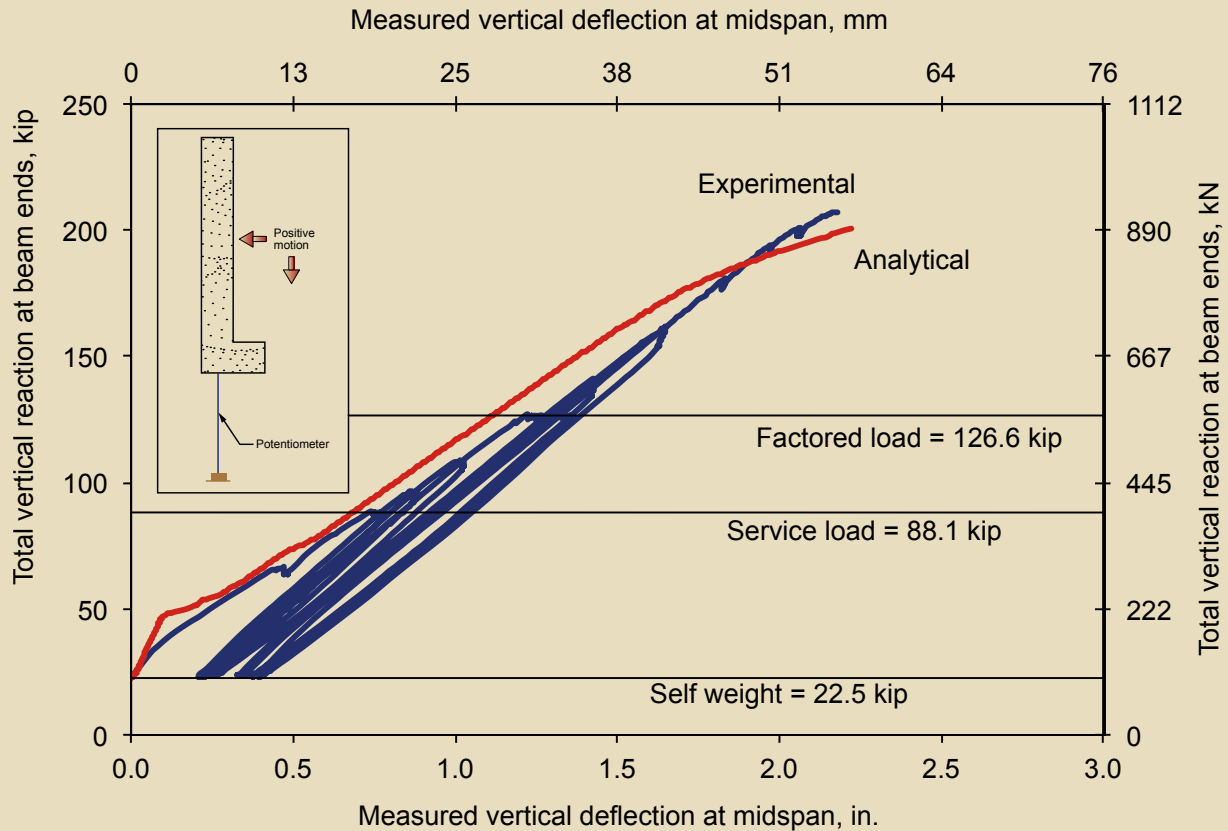


**Figure 4.** Measured and predicted vertical deflections at midspan. Note: 1 in. = 25.4 mm; 1 kip = 4.448 kN.

### Transition region

The transition region extends a distance  $2h$  beyond the end region. Test results indicate that the primary crack angle is approximately 30 deg. Shear and torsion demands are reduced in this region while bending moment demands are increasing compared with the end region.

### Flexure region

The flexure region is defined as the portion of the beam beyond the transition region to the midspan of the beam. The behavior in this region is marked by vertical cracking on the inner and outer web faces due to in- and out-of-plane flexure and by horizontal cracking on the inner web face due to hanger loads. Shear and torsion demands are relatively low, while moment demands are relatively high.

The loading demands considered in the rational model for each region consisted of the factored bending moment  $M_u$ , the factored shear force  $V_u$ , and the factored torque  $T_u$ . Eccentricity  $e$  for the calculation of torsion should be considered from the point of load application to the center of the web. Flexure design should follow the recommendations in the *PCI Design Handbook*.

### Proposed rational model for resisting the applied torsion $T_u$

The vertical eccentric loads acting on a slender spandrel beam produce torque acting about the longitudinal axis of the beam. The torsion demand  $T_u$  is calculated by multiplying the applied factored ledge loads by the distance from the applied load to the center of the web. The  $T_u$  vector at any diagonal crack can be resolved into two equivalent orthogonal vectors (Fig. 7). One component of the torque vector, defined in the analysis as  $T_{ub}$ , will act to bend the spandrel web out of plane about the diagonal axis defined by the diagonal crack angle  $\theta$  (Eq. [1]). The second component of the torque vector, defined in the analysis as  $T_{ut}$ , acts to twist the web about an axis perpendicular to that diagonal crack (Eq. [2]).

$$T_{ub} = T_u \cos \theta \quad (1)$$

$$T_{ut} = T_u \sin \theta \quad (2)$$

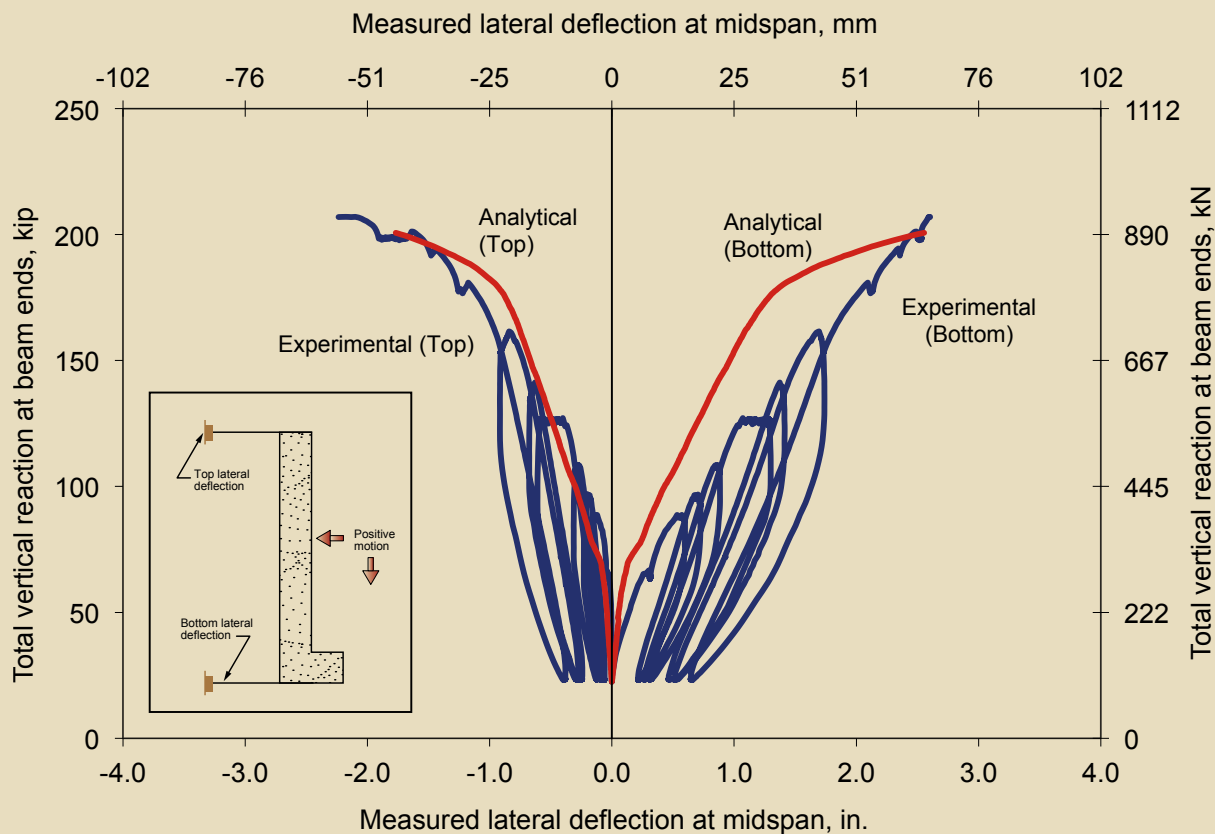


Figure 5. Measured and predicted lateral deflections at midspan. Note: 1 in. = 25.4 mm; 1 kip = 4.448 kN.

### Designing for the plate-bending component of torsion $T_{ub}$

Equation (1) provides the factored out-of-plane bending moment demand about the diagonal axis defined by angle  $\theta$ . The resistance to  $T_{ub}$  is developed by plate bending in the spandrel web. The nominal resisting moment can be closely determined by Eq. (3).

$$T_{ub} = A_s^* f_y d_w \quad (3)$$

where

$T_{ub}$  = plate-bending component of torsion

$A_s^*$  = total area of steel required on the inner web face crossing the critical diagonal crack in a direction perpendicular to the crack

$f_y$  = yield stress of the inner-face reinforcing steel

$d_w$  = effective depth from the outer surface of the web to the centroid of the combined horizontal and vertical steel reinforcement of the web; usually taken as web thickness less concrete cover less the diameter of the

inner-face vertical steel bars

The lateral bending resistance must satisfy the lateral bending demand (Eq. [4]).

$$T_{ub} \leq \phi_f T_{nb} \quad (4)$$

where

$\phi_f$  = strength reduction factor for flexure = 0.9

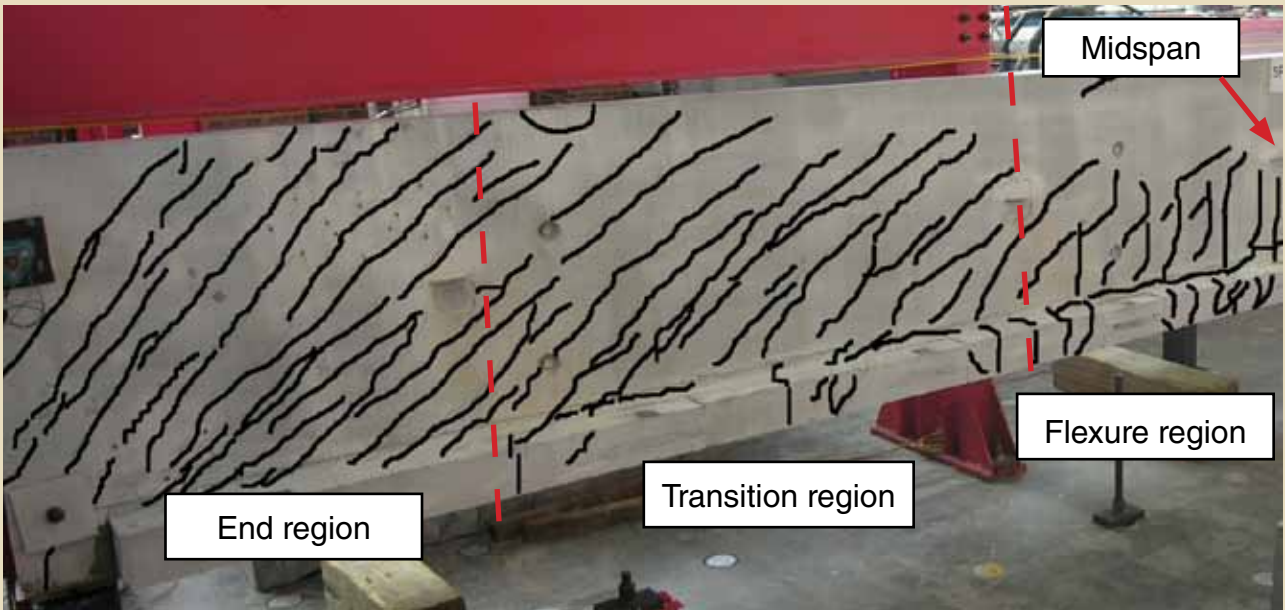
$T_{nb}$  = nominal plate-bending resistance of the web

Combining Eq. (1), (3), and (4) into Eq. (5) results in the total required area of steel  $A_{s,s}^*$ .

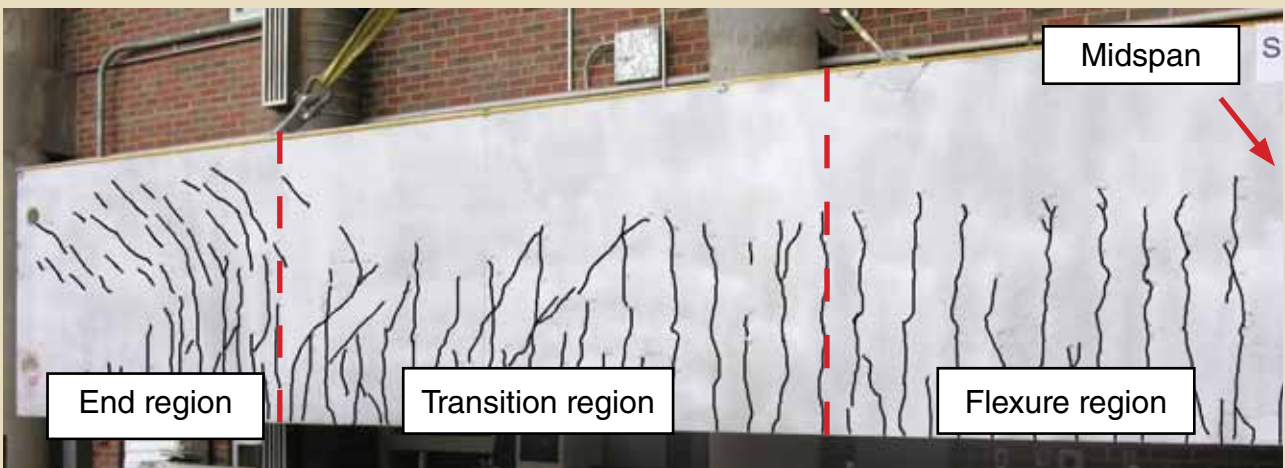
$$A_s^* \geq \frac{T_u \cos \theta}{\phi_f f_y d_w} \quad (5)$$

Although  $T_{ub}$  is a component of torsion, the strength reduction factor for flexure is considered appropriate because  $T_{ub}$  is resisted by out-of-plane flexure of the web, which is plate bending.

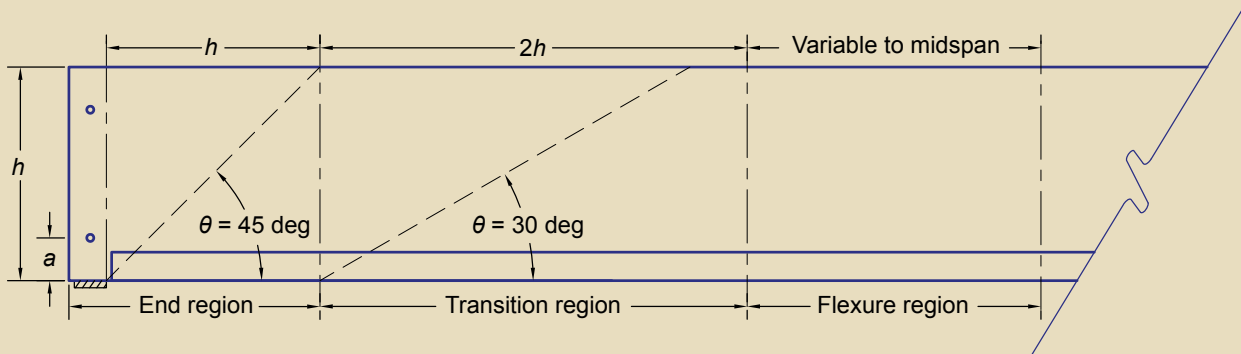
Because the web steel resisting plate bending is usually



Typical inner-face cracking pattern



Typical outer-face cracking pattern



Generic regions of behavior identified in rational model

**Figure 6.** Inspection of the cracking pattern of all tested slender spandrel beams loaded to failure allowed for identification of three distinct zones: end region, transition region, and flexure region. Note:  $a$  = vertical distance from bottom of spandrel to center of lower tieback connection;  $h$  = height of spandrel;  $\theta$  = angle of critical diagonal crack for region under consideration with respect to horizontal.

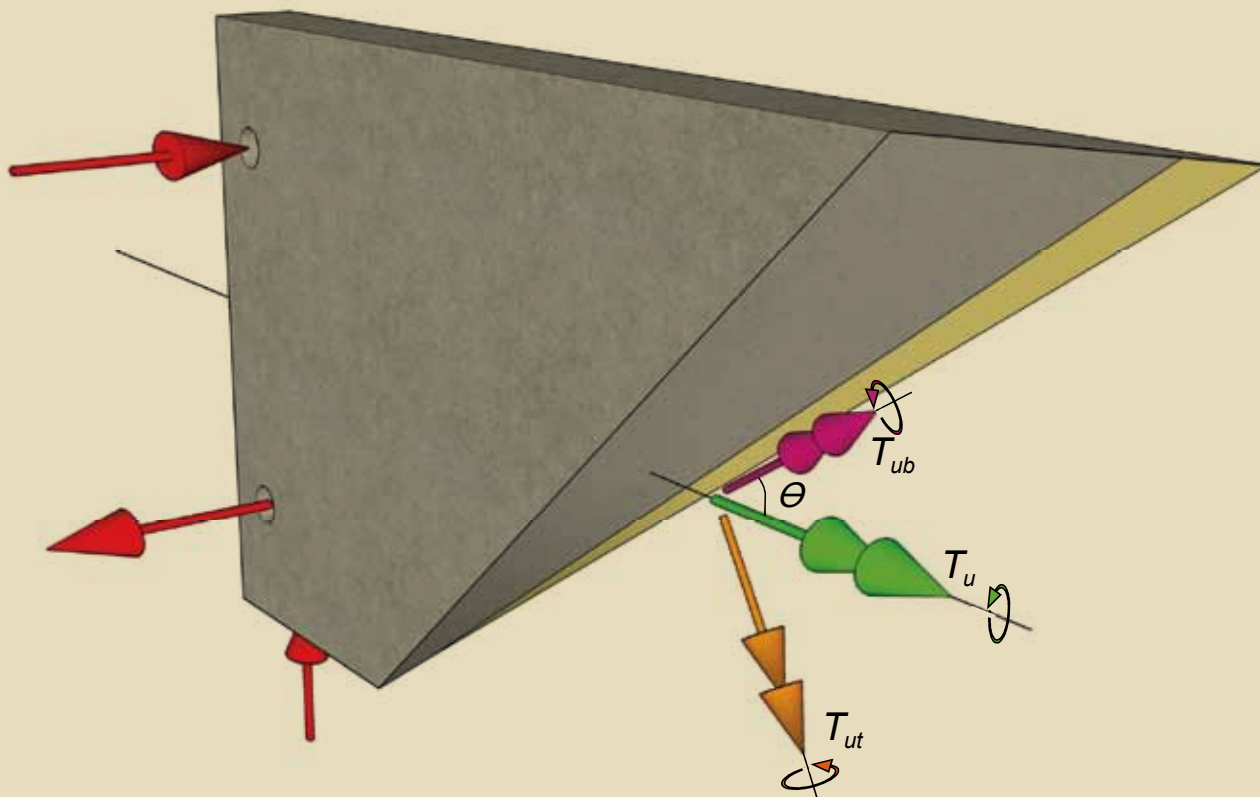


**Figure 7.** Components of applied torque along diagonal crack within end region. Note: The double-headed torque vectors indicate moments according to the right-hand rule.  $T_u$  = factored torque;  $T_{ub}$  = plate-bending component of torsion;  $T_{ut}$  = twisting component of torsion;  $\theta$  = angle of critical diagonal crack for region under consideration with respect to horizontal.

orthogonal to the beam (not perpendicular to a crack), the total required area must be expressed in terms of vertical steel and longitudinal steel. The total required area of vertical steel crossing the diagonal crack  $A_{sv}$  can be determined by Eq. (6).

$$A_{sv} = A_s'' \cos \theta \quad (6)$$

Using Eq. (5) and (6), the required  $A_{sv}$  can be determined by Eq. (7).

$$A_{sv} \geq \frac{T_u \cos^2 \theta}{\phi_f f_y d_w} \quad (7)$$

Similarly, the total required area of longitudinal steel on the inner face to resist plate bending  $A_{sl}$  can be determined by Eq. (8).

$$A_{sl} \geq \frac{T_u \cos \theta \sin \theta}{\phi_f f_y d_w} \quad (8)$$

The area of vertical steel required to resist plate bending  $A_{sv}$  over the horizontal crack projection  $l_{ch}$  can be determined by Eq. (9).

$$l_{ch} \geq \frac{h}{\tan \theta} \quad (9)$$

The required area of plate-bending reinforcement distributed over the horizontal crack projection  $A_{sv}/s$  can be determined by Eq. (10).

$$A_{sv}/s \geq \frac{T_u \cos \theta \sin \theta}{\phi_f f_y d_w h} \quad (10)$$

Similarly, the distributed longitudinal steel required on the inner web face for plate bending  $A_{sl}/s$  can be determined by Eq. (11).

$$A_{sl}/s \geq \frac{T_u \cos \theta \sin \theta}{\phi_f f_y d_w h} \quad (11)$$

Equations (10) and (11) are identical irrespective of crack angle or beam region. The required vertical plate-bending steel distributed over the horizontal crack projection equals the required horizontal plate-bending steel distributed over the vertical crack projection in a given beam region.  $A_{sl}$

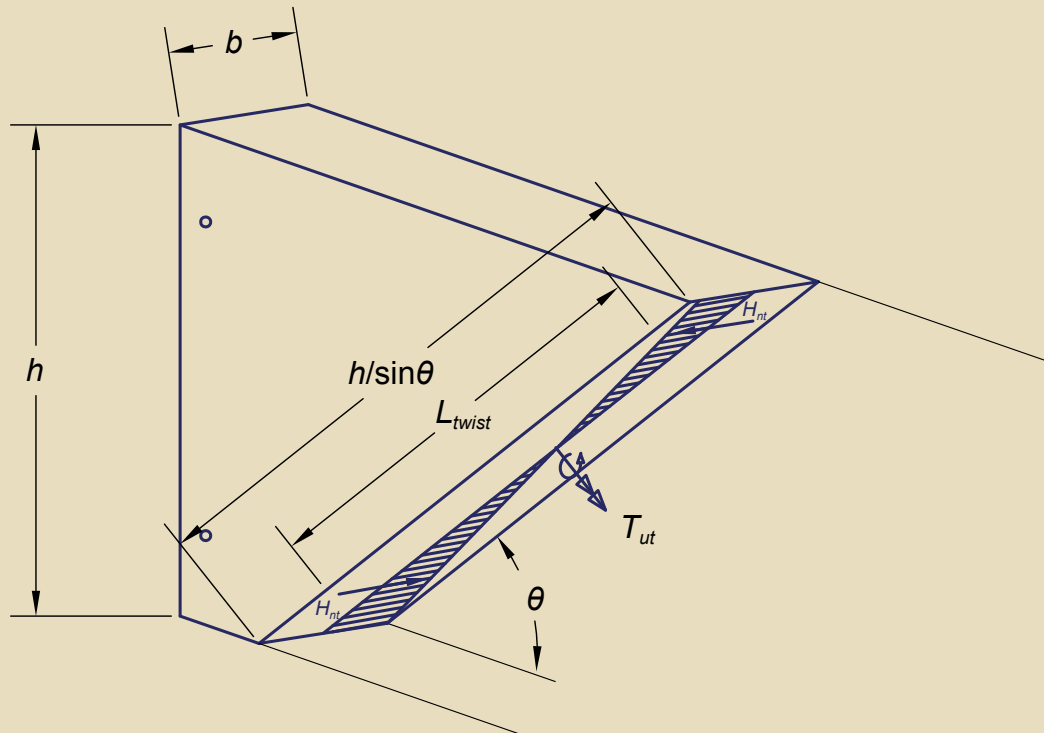


**Figure 8.** Linear distribution of shear stresses on inclined cross section. Note:  $b$  = thickness of web;  $h$  = height of spandrel;  $H_{nt}$  = out-of-plane force resultants;  $L_{twist}$  = lever arm;  $T_{ut}$  = twisting component of torsion;  $\theta$  = critical diagonal crack angle for region under consideration with respect to horizontal.

and  $A_{sv}$  should be calculated for each region at the point of maximum torsion  $T_u$  in that region. In the end region, not all possible diagonal cracks intersect the bottom of the beam. Therefore, it is appropriate to consider a diagonal crack extending upward from the lower lateral tieback, where crack projections would be calculated using the distance  $h - a$  in place of  $h$ . Further details are presented in the technical report.<sup>2</sup>

The vertical reinforcement resisting plate bending  $A_{sv}$  is based on the assumption that the inner-face web steel yields under the effect of the applied factored plate-bending moment  $T_{ub}$ . Calculation indicates that, in practical designs, the reinforcement requirements for plate bending are substantially less than the tension-controlled limit. Thus, plate-bending web steel will yield with significant ductility required for tension-controlled failure, and a value of 0.9 for  $\phi_f$  is justified.

### Designing for the twisting component of torsion $T_{ut}$

The proposed rational model requires that the twisting resistance of the cracked section  $\phi_s T_{nt}$  (where  $\phi_s$  is the strength reduction factor for shear and  $T_{nt}$  is the nominal twist resistance of the section) exceed the twisting demand, with  $\phi_s$  equal to 0.75, according to the *Building Code Requirements for Structural Concrete (ACI 318-08)* and

*Commentary (ACI 318R-08)*<sup>8</sup> recommendation for torsion design. The twist demand must be resisted by a cross section through a diagonal crack, normal to the  $T_{ut}$  vector, having dimensions of  $h/\sin \theta$  and thickness  $b$  (Fig. 8).

Evaluation of the twisting resistance in slender spandrel beams is based on the well-accepted mechanism used to transfer unbalanced moments from reinforced concrete slabs to columns. In the case of a column-slab interface, ACI-318-08 section 11.11.7.2 recommends that the shear stress “shall vary linearly about the centroid of the critical section.” The same concept of linear shear distribution is applied to the inclined cross section of a slender spandrel beam (Fig. 8). The linear model assumes a shear-stress distribution with a maximum value at the extreme end of the section. More complex models for twisting resistance were evaluated using rational models and FEMs. The complex models and finite element analysis closely match the linear approximation, as discussed in the technical report.<sup>2</sup> In all cases, the reduced nominal twisting resistance must exceed the factored twist demand, as shown in Eq. (12).

$$T_{ut} \leq \phi T_{nt} \quad (12)$$

Based on the linear stress distribution in Fig. 8, the out-of-plane resultant forces  $H_{nt}$  are separated by a distance  $L_{twist}$

equal to 2/3 the height of the diagonal crack. The magnitude of these resultant forces is determined in Eq. (13).

$$H_{nt} = \left( \frac{1}{2} \frac{h}{\sin \theta} \right) \frac{1}{2} d_w X \sqrt{f'_c} \quad (13)$$

where

$H_{nt}$  = out-of-plane force resultants from a linear shear-stress distribution

$f'_c$  = specified concrete compressive strength

$X$  = out-of-plane shear-stress coefficient (calibrated later in this paper from experimental data)

$X\sqrt{f'_c}$  = maximum shear stress of the linear distribution (calibrated from the experimental data later in this paper)

Accordingly, the nominal twist resistance of the section  $T_{nt}$  can be evaluated as the product of  $H_{nt}$  and  $L_{twist}$  (Eq. [14]).

$$T_{nt} = X\sqrt{f'_c} \frac{1}{6} \frac{h^2}{\sin^2 \theta} d_w \quad (14)$$

To ensure that the twisting resistance according to the linear model exceeds or equals the applied factored torque demand, Eq. (15) should be satisfied. Equation (15) is derived by substituting Eq. (14) and (2) into Eq. (12).

$$T_u \leq \phi_s X \sqrt{f'_c} \frac{1}{6} \frac{h^2}{\sin^3 \theta} d_w \quad (15)$$

where

$$\phi_s = 0.75$$

### Calibration of the twist-resistance model

Of the 16 tested beams, seven failed in out-of-plane modes in their end regions. For each of these seven beams, the measured lateral reactions at failure were used to calculate the out-of-plane shear stresses resisted by a given beam just before failure. It is recognized that there are interactions among the flexural, shear, and torsional stresses on the failure plane. Because the proposed twist resistance is calibrated to the measured test data, it accounts for the effects of the flexural stress and the vertical shear and torsional stresses. However, the proposed method neglects the effect of the torsional stress on the vertical shear stress based on the experimental evidence for beams tested.

The twist-resistance model was calibrated by first determining the torsion acting on the end region of a given beam at failure. For each tested beam, all lateral forces were included to determine the twisting moment at failure  $T'_t$ . Lateral forces not directly measured during the tests were evaluated by considering the equilibrium of the beam as a whole about a selected origin, point O (Fig. 9).

The sum of lateral forces at the deck connections  $\Sigma H_2$  and the friction coefficient  $\mu$  were determined by considering moment equilibrium about point O and force equilibrium in the horizontal direction. The analysis was performed for each of the seven beams that failed in its end region. The range of calculated friction coefficients corresponds well to the value of 0.05 determined by the nonlinear finite element analysis described previously. In addition, the calculated values correspond well to the range published in the *PCI Design Handbook* for Teflon-coated bearing pads similar to those used in the tests.

With all lateral forces determined, the twisting component of torsion resisted by each beam at failure was evaluated. Figure 10 shows a free body diagram taken along a 45 deg crack plane extending upward from the face of the support (line 1-1 in the figure). All dimensions are known from the geometry of a given beam, and all forces were measured or determined from equilibrium. There are no deck connections to the left of crack plane 1-1; therefore, the deck connection forces  $H_2$  do not appear in the free body diagram to the left of the crack.

The out-of-plane shear stress induced by the twisting moment at failure  $T'_t$  was assumed to be distributed linearly across the selected crack plane 1-1 (Fig. 10). The maximum values at the extremes of the distribution are identified as  $X^* \sqrt{f'_c}$  and  $\bar{X} \sqrt{f'_c}$ , where  $X^*$  is the height of the centroid and  $\bar{X}$  is the extreme value of the stress distribution. The location of the centroid of the twisting moment was determined by an iteration process that satisfied moment equilibrium about the selected centroid and equilibrium of the horizontal forces. The tendency of the vertical reaction to shift inward (toward the ledge) as a spandrel deforms under load was conservatively neglected. Based on the two equilibrium equations, the height of the centroid  $X^*$  and the extreme values of the stress distribution  $\bar{X}$  were determined for each experimental case (Table 1).  $X^*$  and  $\bar{X}$  are related by the linear distribution.

The calculated height of the twist axis  $Z_t$  is consistently just above the midheight of all specimens. Therefore, assuming a balanced linear stress distribution for design is an acceptable approximation.

Given the results in Table 1, a conservative value of 2.4 is recommended for  $X$  in Eq. (15). Because the centroid of the linear distribution assumed for design will be considered at the midheight of the cross section, it is appropriate to compare the selected value of  $X$  to the values of  $X_{avg}$

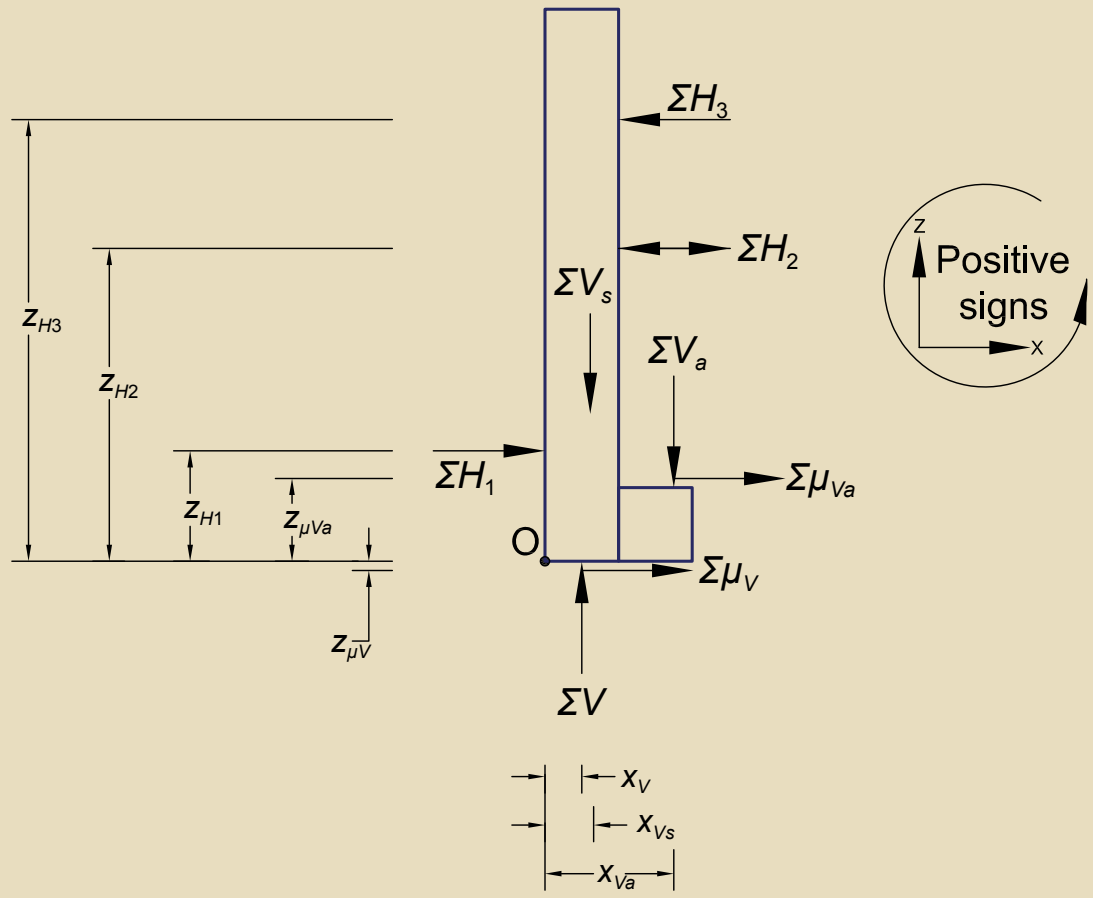


**Figure 9.** Equilibrium of generic slender spandrel beam. Note: 0 = origin;  $X_V$  = distance from outer web face to center of main vertical reaction, estimated to remain at center of the web;  $X_{Va}$  = distance from outer web face to center of ledge reactions, estimated to remain at center of ledge bearing pads;  $X_{Vs}$  = distance from outer web face to center of self-weight reaction, estimated to remain at center of gravity;  $Z_{H1}$  = height of lower lateral reaction;  $Z_{H2}$  = height of te deck connection;  $Z_{H3}$  = height of upper lateral reaction;  $Z_{\mu V}$  = height to Teflon surface of main bearing pad;  $Z_{\mu Va}$  = height to Teflon surface of ledge (or corbel) bearing pad;  $\Sigma H_1$  = sum of measured lower lateral reactions at failure;  $\Sigma H_2$  = sum of lateral forces at deck connections;  $\Sigma H_3$  = sum of measured upper lateral reactions at failure;  $\Sigma V$  = sum of measured vertical reactions at failure;  $\Sigma V_a$  = sum of loads applied to spandrel by double-tee decks and jacks;  $\Sigma V_s$  = self-weight of spandrel beam;  $\Sigma \mu_V$  = sum of lateral forces at main vertical bearing due to friction;  $\Sigma \mu_{Va}$  = sum of lateral forces at ledge (or corbel) due to friction.

(averages of  $X^*$  and  $\bar{X}$  [Table 1]). Selecting a value below  $X_{avg}$  is a safe choice for design, especially considering the conservative nature of the linear distribution and the assumptions made in the calibration.

**Figure 11** plots the ratio of twisting moment at failure to nominal twisting capacity for all seven spandrels that failed in their end regions. These seven spandrel beams were specially configured to induce end-region failure modes by over-reinforcing other controlling failure modes.<sup>1</sup> The plot shows that Eq. (15), with a value of 2.4 for  $X$ , conservatively predicts the twisting capacity of each tested beam. Thus, Eq. (15) is recommended for design with 2.4 for the value of  $X$ . This recommendation provides a conservative prediction of the twisting moment capacity of a slender spandrel and is consistent with the historical association (ACI 318-71<sup>9</sup>) of  $2.4\sqrt{f'_c}$  with torsion. Thus, Eq. (16) gives the proposed twist resistance using the linear shear-stress distribution model.

$$T_u \leq \phi_s \left( 2.4\sqrt{f'_c} \frac{d_w h^2}{6 \sin^3 \theta} \right) \quad (16)$$

### Shear and torsion stresses

Due to the loading and support conditions, shear and torsion stresses act in the same direction on the inner web face (the face on the ledge or corbel side) but oppose each other on the outer web face<sup>10</sup> (**Fig. 12**). The concrete on the inner face is more vulnerable to diagonal cracking. This behavior is clearly identified by experimental cracking patterns<sup>1</sup> and is verified by linear finite element analysis presented in the technical research report.<sup>2</sup>

### Designing for the applied shear

As discussed previously, the rational model considers the design of shear and torsion independently. Thus, design

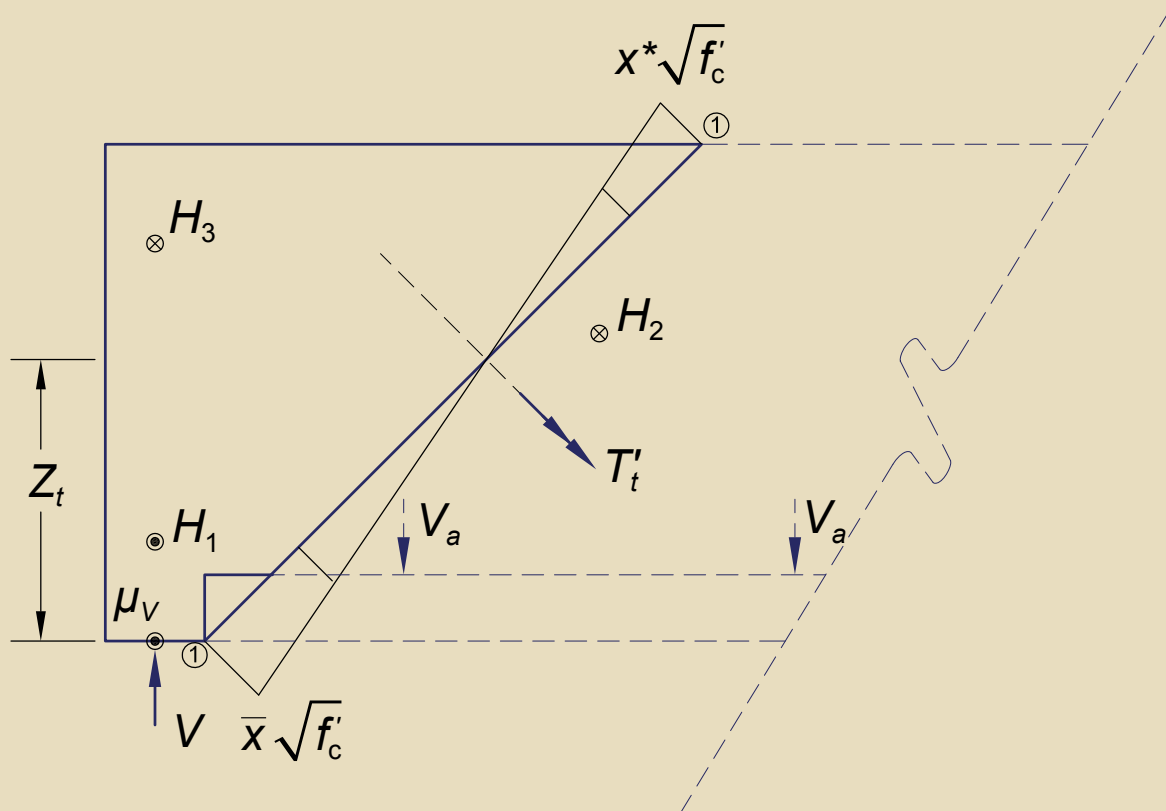


**Figure 10.** Forces contributing to torque on a slender spandrel end region. Note: Forces acting into the page are identified by a circle with a cross, while forces acting out of the page are identified by a circle with a dot.  $f'_c$  = specified concrete compressive strength;  $H_1$  = measured lower lateral tieback reaction;  $H_2$  = deck connection forces;  $H_3$  = measured upper lateral tieback reaction;  $T'_t$  = torque at failure;  $V$  = measured main vertical end reaction;  $V_a$  = experimentally applied stem loads;  $X^*$  = height of centroid;  $\bar{X}$  = extreme values of stress distribution;  $Z_t$  = height of twist axis;  $\mu$  = friction coefficient.

for shear should follow traditional practice. Equation (17) determines the uniformly distributed vertical shear reinforcement  $A_v/s$  required at a given cross section to resist the factored shear force  $V_u$ .

$$A_v/s \geq \frac{V_u/\phi_s - V_c}{f_y d} \quad (17)$$

where

$$\phi_s = 0.75$$

$V_c$  = nominal concrete shear strength equal to the lesser of  $V_{ci}$  or  $V_{cw}$ , as given by Eq. (11-11) and (11-12) of ACI 318-08

$V_{ci}$  = nominal shear strength provided by concrete when diagonal cracking results from combined shear and moment

$V_{cw}$  = nominal shear strength provided by concrete when diagonal cracking results from high principal tensile stress in the web

The minimum requirements for area of shear reinforcement  $A_v$  specified by ACI 318-08 may control over Eq. (17).

### Proportioning the web reinforcement

The previously calculated quantities of steel reinforcement required to resist torsion and shear must be provided in the spandrel web according to the nature of shear and torsion stresses illustrated in Fig. 12.

The total quantity of distributed vertical steel required on the inner web face  $A_{si}/s$  is the quantity required for the plate-bending component of torsion plus half of the total quantity required for shear (Eq. [18]).

$$A_{si}/s \geq \frac{T_u \cos \theta \sin \theta}{\phi_f f_y d_w h} + \frac{V_u/\phi_s - V_c}{2f_y d} \quad (18)$$

where

$d$  = distance from the extreme compression fiber to the centroid of the longitudinal reinforcement



**Table 1.** Results from twist model calibration

Test specimen	$Z_t$ , in.	$X^*$ , psi/ $\sqrt{f'_c}$	$\bar{X}$ , psi/ $\sqrt{f'_c}$	$X_{avg}$ , psi/ $\sqrt{f'_c}$
SP3.8L60.45.P.O.E	34.5	2.36	3.19	2.77
SP4.8L60.45.P.O.E	33.9	2.02	2.62	2.32
SP10.8L60.45.R.O.E	36.7	2.48	3.91	3.20
SP12.8L60.45.P.O.E	35.9	1.90	2.83	2.36
SP17.8CB60.45.P.O.E	37.0	1.82	2.94	2.38
SP18.8CB60.45.P.S.E	36.8	2.17	3.45	2.81
SP20.10L46.45.P.O.E	26.4	2.11	2.83	2.47
Mean				2.62
Minimum				2.32
Standard deviation				0.32

Note:  $X^*$  = height of the centroid;  $\bar{X}$  = extreme values of stress distribution;  $X_{avg}$  = average of  $X^*$  and  $\bar{X}$ ;  $Z_t$  = height of twist axis.  
 1 in. = 25.4 mm; 1 psi = 6.895 kPa.

The remaining half of the required shear reinforcement is allocated to the outer spandrel face where shear and torsion stresses oppose each other. On the outer face, the vertical component of the plate-bending compressive force reduces the amount of required vertical reinforcement for shear (Fig. 13).

Thus, the total distributed vertical reinforcement required on the outer web face  $A_{so}$  can be theoretically reduced by the component of vertical plate bending (Eq. [19]), provided that the total amount of transverse reinforcement in the beam is sufficient for shear. However, it is recommended that  $A_{so}$  be provided as half of  $A_v$ .

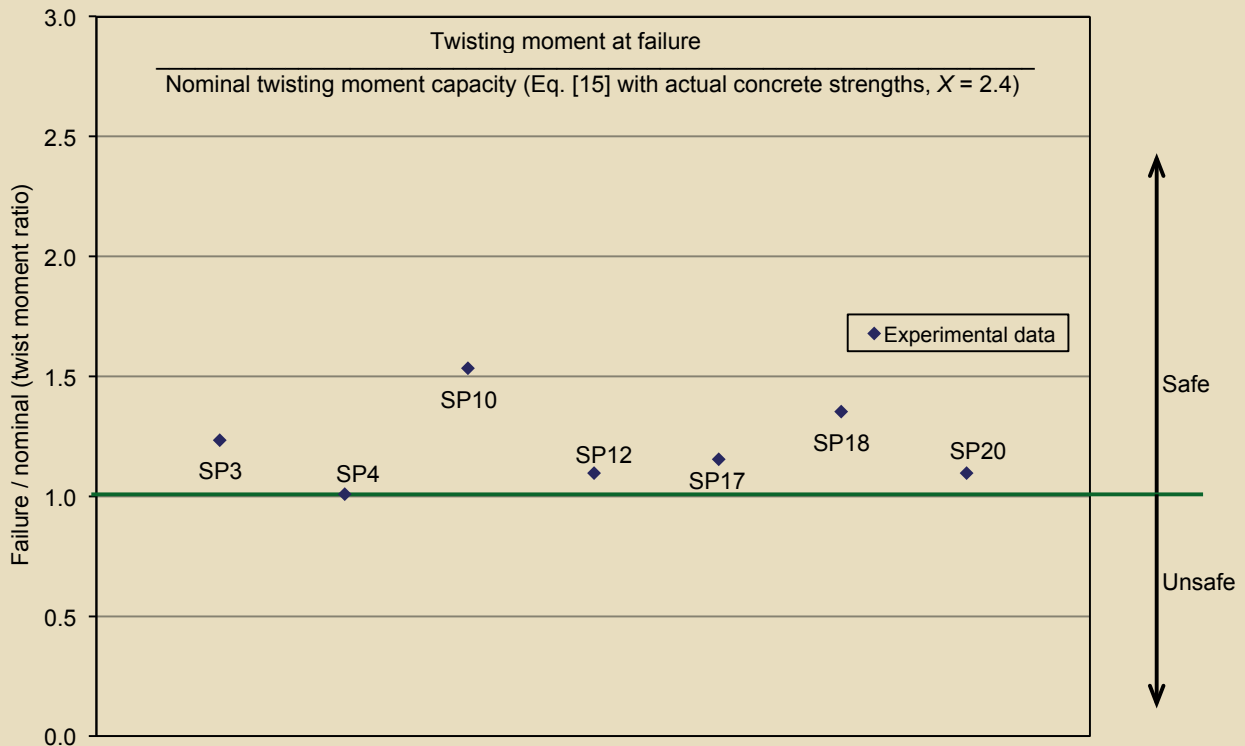


**Figure 11.** Ratio of failure twisting moment to proposed nominal twisting moment.

## Shear                      Torsion                      Combined

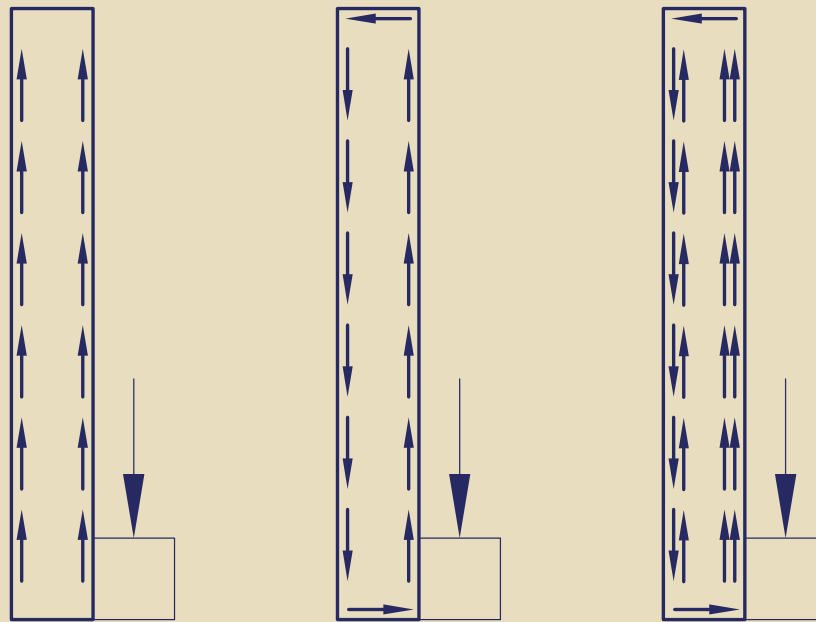


**Figure 12.** Directions of shear and torsional stresses acting on slender spandrel cross section.

$$A_{so}/s \geq \frac{V_u/\phi_s - V_c}{2f_y d} - \frac{T_u \cos \theta \sin \theta}{f_y d_w h} \quad (\text{in.}^2/\text{in.}) \quad (19)$$

On the outer web face, plate bending about a crack extending downward from the top lateral reaction can, in theory, control a design; however, this orthogonal plate bending is counteracted by vertical shear. Failure about this potential plane could only develop if torsional stresses, acting upward on the outer face, greatly exceeded the shear stresses, acting downward. Further details and analysis related to orthogonal plate bending are presented in the technical report.<sup>2</sup>

The longitudinal steel  $A_{sl}$  calculated by Eq. (8) is to be provided on both the inner and the outer web faces. Providing longitudinal steel on the outer face protects against possible plate bending on the outer face. In addition, longitudinal steel provides dowel forces beneficial to twist resistance, particularly in the end region.

### Potential additional failure modes

Other reinforcement requirements may control the design of web reinforcement and must be checked according to procedures specified in the *PCI Design Handbook*. By experience, it was found that hanger steel requirements will often control the design of vertical reinforcement on the inner web face, especially outside of the end region. Hanger steel requirements need not be combined with the vertical

steel required for shear and torsion. Only the greater of the two should be used.

### First cracking load

The anticipated load causing initial cracking in the end region of a slender spandrel beam is often of interest to the designer. While minor hairline cracking is usually not a concern from a structural or durability standpoint, it may be desirable to minimize or eliminate such cracking in cases where aesthetics are relevant. The first cracking load will be the same whether open or closed transverse web reinforcement is used.

Equation (20) gives the diagonal tensile stress due to shear of a slender spandrel  $f_{cr1}$ .

$$f_{cr1} = \frac{3V}{2bh} \quad (20)$$

where

$f_{cr1}$  = diagonal tension stress due to shear

$V$  = the applied shear force at the level of interest

$b$  = width of web

$h$  = height of the spandrel

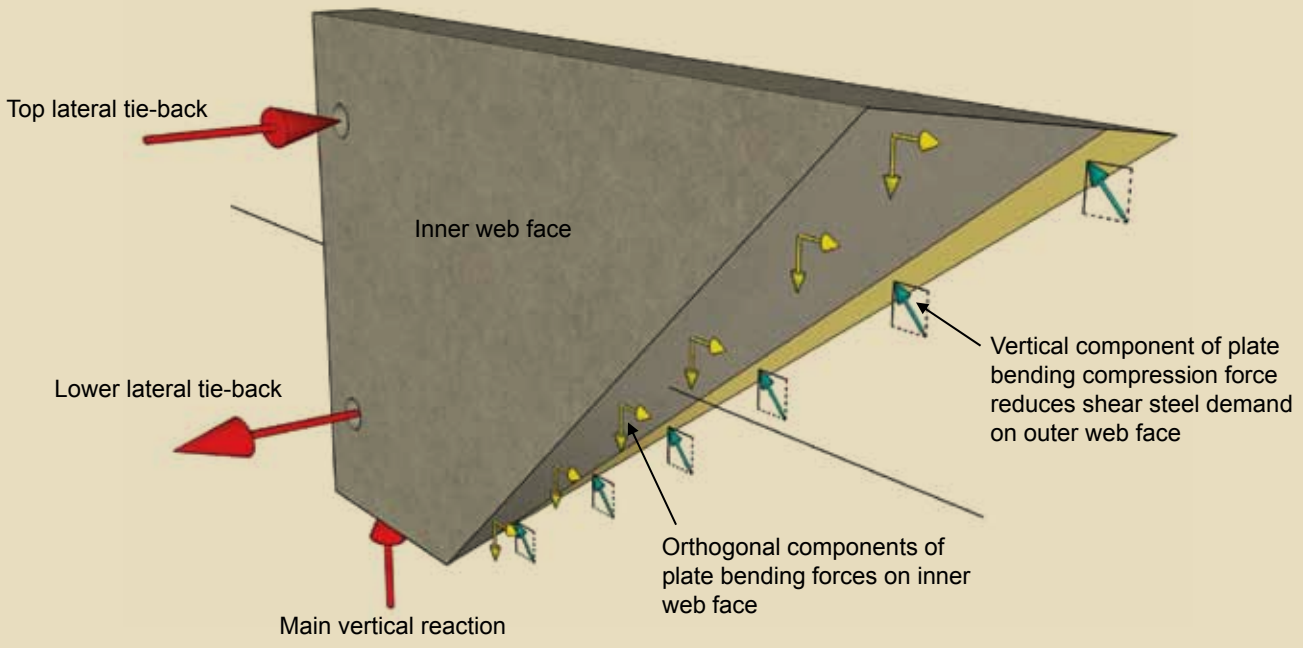


**Figure 13.** Compression on outer web face due to plate bending.

Equation (21) calculates the diagonal tensile stress due to plate bending of a slender spandrel.

$$f_{cr2} = \frac{3T}{b^2h} = \frac{3Ve}{b^2h} \quad (21)$$

where

$f_{cr2}$  = diagonal tension stress due to plate bending

$T$  = applied torque

$e$  = eccentricity contributing to torsion

Combining Eq. (20) and (21) and assuming a limiting tensile stress of concrete of  $6\sqrt{f'_c}$ , Eq. (22) can determine the shear force at cracking  $V_{cr}$ .

$$V_{cr} = \left[ \frac{4\sqrt{f'_c}}{(1 + 2e/b)} \right] bh \quad (22)$$

Comparison with experimental data indicates that Eq. (22) provides a conservative estimate of the load at which cracking is first likely to appear. First cracking loads can be increased by increasing the web thickness, increasing the concrete strength, or distributing prestressing force through the height of the web. Prestressing force concentrated only near the bottom of the section is not effective in controlling diagonal cracks near the support.

In actual structures, cracking can be influenced by handling, curing conditions, thermal exposure, and other factors. Also, concentration of stresses near the bearing area increases the likelihood of cracking just inside the support. As such, cracking may occur sooner than expected. However, if designed as recommended herein, end-region diagonal cracks will be narrow and will not adversely affect strength or durability. The aesthetic impact should also be minimal.

### Proposed simplified design guidelines

To assist the designer, a step-by-step simplified design procedure was developed based on the rational model. The procedure is intended for slender precast concrete spandrel beams subject to the following restrictions:

- A simply supported precast concrete spandrel is loaded along the bottom edge of the web.
- Normalweight concrete is used.
- The web is laterally restrained at two points at each end.
- Applied loads are evenly spaced along the bottom edge of the web.
- The aspect ratio (height divided by web thickness) is equal to or more than 4.6.

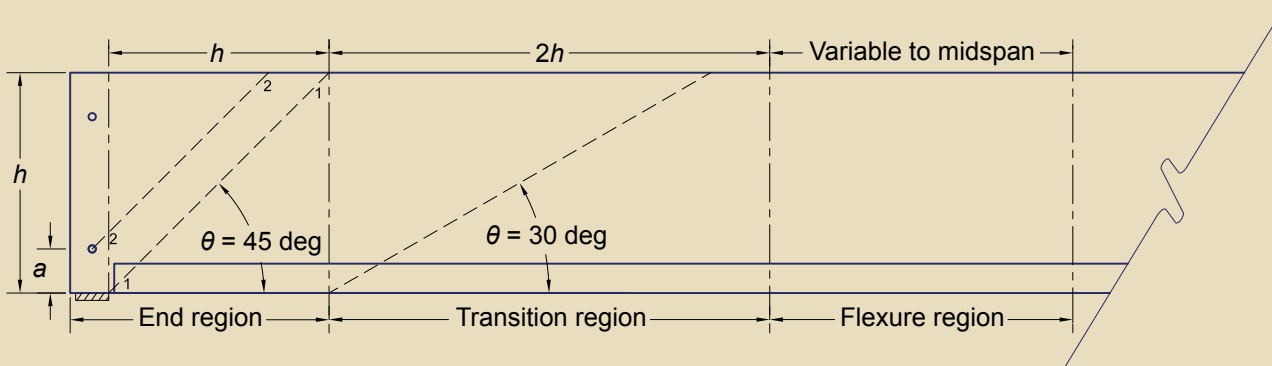


**Figure 14.** Regions of slender spandrel beam. Note: end region = region from end of beam to distance  $h$  beyond inner face of support; transition region =  $2h$  beyond end region; flexure region = remainder of beam;  $a$  = height from bottom of spandrel to center of lower lateral tieback;  $h$  = height of web;  $\theta$  = critical diagonal crack angle for region under consideration with respect to horizontal = 45 deg for end region = 30 deg for transition region.

### Step 1: Determine the loading demands

Construct the factored bending moment, shear, and torsion diagrams. Eccentricity for calculating torsion should be taken from the point of applied load to the center of the web.

### Step 2: Divide the slender spandrel into the three regions shown in Fig. 14

### Step 3: Verify that the cross section can sustain the twisting component of torsion

Verify that the maximum torque  $T_u$  in the end region does not exceed the twist limit for this region by considering Eq. (23).

With  $\theta$  taken as 45 deg for the end region, Eq. (16) becomes Eq. (23).

$$T_u \leq \phi_s \left( 1.13 \sqrt{f'_c} d_w h^2 \right) \quad (23)$$

where

$$\phi_s = 0.75$$

Conservatively, Eq. (23) can also be used to check twist capacity in the transition region. However, twist in the transition region will not control the design for a simply supported beam with a uniform cross section. Similarly, there is no need to check the twist limit in the flexure region. Because the proposed twist resistance is calibrated to the measured test data, it accounts for the effects of the flexural stress and the vertical shear and torsional stresses.

If the lateral end reactions are spaced vertically at least  $0.6h$ , a check for twist resistance on a secondary failure plane in the end region (line 2-2 in Fig. 14) is not required. Otherwise a check is necessary by using the height of the section above the lower connection (distance  $h - a$ , where  $a$  is the vertical distance from the bottom of a spandrel to the center of the lower tieback connection) in Eq. (23) in lieu of  $h$ . Calculations involving the transition region would still use the full section height  $h$ . If this check for the twisting component of torsion is not satisfied, the concrete strength or cross-section dimensions would have to be increased; otherwise, closed reinforcement would have to be used.

### Step 4: Design the beam for flexure

Design and proportion the longitudinal steel reinforcement (mild or prestressed) in accordance with section 4.2 of the *PCI Design Handbook*.

### Step 5: Calculate the required shear steel at all sections along the beam

Design the beam for shear according to all provisions in section 4.3 of the *PCI Design Handbook*. For the vertical shear design in this step, ignore eccentricity.

Determine the amount of vertical shear reinforcement required per unit length ( $A_v/s$ ) at all locations along the length of the beam.  $A_v$  will likely change at each applied point load along the ledge and will also be influenced by the development of prestressing strands in the end region. All requirements for minimum  $A_v$  still apply.

The proposed method neglects the effect of the torsional stress on the vertical shear stress based on successful performance of the test specimens, which were designed without consideration of the influence of torsion on shear strength. However, Zia and Hsu<sup>7</sup> indicated that torsion reduces shear strength, especially in compact sections. As



such, this procedure should only be applied to precast concrete spandrel beams with an aspect ratio of 4.6 or more.

### Step 6: Calculate the vertical reinforcement required on the inner web face to resist the plate-bending component of torsion

Consider plate bending in the end region and in the transition region (Fig. 14). There is no need to consider plate bending in the flexure region.

Use Eq. (24) and Eq. (25) to calculate the distributed quantity of vertical steel (in.<sup>2</sup>/in.) required to resist plate bending for the end region and transition region, respectively, using the maximum  $T_u$  from each region. These equations are the same as Eq. (10) with  $\theta$  taken as 45 deg (for the end region) or 30 deg (for the transition region).

For the end region:

$$A_{sv}/s \geq \frac{T_u}{2\phi_f f_y d_w h} \quad (24)$$

Units:  $A_{sv}$  (in.<sup>2</sup>),  $s$  (in.),  $T_u$  (lb-in.),  $h$  (in.),  $d_w$  (in.),  $f_y$  (psi),  $\phi_f = 0.9$

For the transition region:

$$A_{sv}/s \geq \frac{T_u}{2.3\phi_f f_y d_w h} \quad (25)$$

Units:  $A_{sv}$  (in.<sup>2</sup>),  $s$  (in.),  $T_u$  (lb-in.),  $h$  (in.),  $d_w$  (in.),  $f_y$  (psi),  $\phi_f = 0.9$

### Step 7: Proportion the vertical steel on the inner web face

Provide vertical steel on the inner web face (ledge or corbel side) to satisfy Eq. (26) at all locations.

$$A_{sl}/s \geq \left( A_{sv} + \frac{1}{2}A_v \right) / s \quad (26)$$

Units:  $A_{sv}$  (in.<sup>2</sup>),  $A_v$  (in.<sup>2</sup>)

Additional requirements, such as hanger steel or impact steel, may control the design of the inner-face web reinforcement. Provide hanger steel or the steel required by Eq. (26), whichever is greater.

### Step 8: Check the plate-bending capacity about line 2-2 in the end region

Plate bending about line 2-2 may be more critical than plate bending about line 1-1 in the end region (Fig. 14). Whether line 2-2 is critical for plate bending depends on the location of the lateral tieback reactions and on the quantity of vertical shear steel  $A_v$ . After proportioning vertical steel in step 7, verify that the total quantity of vertical steel crossing line 2-2 on the inner face  $A_{sv2}$  exceeds Eq. (27).

$$A_{sv2} \geq \frac{T_u}{\phi_f 2f_y d_w} \quad (27)$$

### Step 9: Proportion the vertical steel on the outer web face

Provide vertical steel on the outer web face to satisfy Eq. (28) at all locations.

$$A_{so} \geq \frac{1}{2}A_v \quad (28)$$

### Step 10: Calculate the longitudinal reinforcement required to resist the plate-bending component of torsion

Calculate the total area of longitudinal steel required to resist plate bending with Eq. (29) and Eq. (30) for the end region and transition region, respectively, using the maximum  $T_u$  from each region. There is no need to consider plate bending in the flexure region. These equations are the same as Eq. (8) with  $\theta$  taken as 45 deg for the end region and 30 deg for the transition region.

For the end region:

$$A_{sl} \geq \frac{T_u}{2\phi_f f_y d_w} \quad (29)$$

For the transition region:

$$A_{sl} \geq \frac{T_u}{2.3\phi_f f_y d_w} \quad (30)$$

Units:  $A_{sl}$  (in.<sup>2</sup>),  $f_c'$  (psi),  $h$  (in.),  $d_w$  (in.),  $T_u$  (lb-in.),  $f_y$  (psi),  $\phi_f = 0.9$

### Step 11: Proportion the longitudinal web steel for plate bending

Provide the required longitudinal web steel (from Eq. [29] and [30]) on both the inner and outer web faces. The longitudinal bars should be developed at the start of each region

and extend for the full length of that region. Generally, horizontal U-shaped bars are effective in the end regions because they allow for development at the end of the beam.

In the end region, longitudinal steel below the level of the lower lateral reaction should not be counted toward the plate-bending requirement.

In the transition region, fully developed excess longitudinal reinforcement not required for flexure may be used as part of the plate-bending requirement.

## Step 12: Detail the beam

Recommendations in the *PCI Design Handbook* regarding ledge design, connection detailing, hanger steel, vehicular-impact steel, and reinforcement for other possible localized failure modes are to be considered. In addition, it is recommended that continuous bars or strands be placed in the longitudinal direction at all four corners of the web to control the possible cracking from lateral bending away from the ends.

## Step 13: Check service-level cracking

If desired, the load at which diagonal cracking in the end region is first likely to appear may be conservatively estimated according to Eq. (31). In many cases, beams will be cracked at service load, regardless of end-region reinforcement. First cracking load is independent of web reinforcement configuration (that is, open or closed stirrups). The effects of prestressing are ignored in Eq. (31) because some of the prestressing strands are not fully developed across the potential crack.

$$V_{cr} = \left[ \frac{4\sqrt{f'_c}}{(1 + 2e/b)} \right] bh \quad (31)$$

where

$V_{cr}$  = shear force at cracking

## Abstract

A rational design method is recommended for the design of precast concrete slender spandrel beams with aspect ratios greater than or equal to 4.6. The procedure was developed using data from an extensive research program including 16 full-scale tests, extensive finite element modeling, and a rational analysis. It is recommended that the design for shear and torsion of slender precast concrete spandrel beams use the concept of resolving the applied torsion into two orthogonal vectors: a plate-bending component and a twisting component. Equations were presented for evaluating the capacity of a slender precast concrete spandrel

beam to resist both components of torsion. The research demonstrates that slender precast concrete spandrel beams can be safely designed to resist the combined effects of flexure, shear, and torsion without the use of traditional closed web reinforcement. Use of open web reinforcement could greatly reduce reinforcement congestion in the end regions of spandrel beams and provide significant savings in fabrication cost.

## Acknowledgments

This research was sponsored by the PCI Research and Development Committee. The work was overseen by an L-spandrel advisory group chaired by Donald Logan. The authors are grateful for the support and guidance provided by this group throughout all phases of the research. In addition, the authors would like to thank the numerous PCI Producer Members who donated test specimens, materials, and expertise in support of the experimental program.

## References

1. Lucier, G., C. Walter, S. Rizkalla, P. Zia, and G. Klein. 2011. Development of a Rational Design Methodology for Precast Concrete Slender Spandrel Beams: Part 1, Experimental Results. *PCI Journal*, V. 56, No. 2 (Spring): pp. 88–112.
2. Lucier, G., C. Walter, S. Rizkalla, P. Zia, and G. Klein. 2010. Development of a Rational Design Methodology for Precast Slender Spandrel Beams. Technical report no. IS-09-10. Constructed Facilities Laboratory, North Carolina State University, Raleigh, NC.
3. Logan, D. 2007. L-Spandrels: Can Torsional Distress Be Induced by Eccentric Vertical Loading? *PCI Journal*, V. 52, No. 2 (March–April): pp. 46–61.
4. Klein, Gary J. 1986. *Design of Spandrel Beams*. PCI Specially Funded Research and Development program research project no. 5 (PCISFRAD #5). Chicago, IL: PCI.
5. Raths, Charles H. 1984. Spandrel Beam Behavior and Design. *PCI Journal*, V. 29, No. 2 (March–April): pp. 62–131.
6. PCI Industry Handbook Committee. 2004. *PCI Design Handbook: Precast and Prestressed Concrete*. MNL-120. 6th ed. Chicago, IL: PCI.
7. Zia, P., and T. Hsu. 2004. Design for Torsion and Shear in Prestressed Concrete Flexural Members. *PCI Journal*, V. 49, No. 3 (May–June): pp. 34–42.
8. ACI Committee 318. 2008. *Building Requirements for Structural Concrete (ACI 318-08) and Comm-*



tary (ACI 318R-08). Farmington Hills, MI: American Concrete Institute (ACI).

9. ACI Committee 318. 1971. *Building Code Requirements for Structural Concrete (ACI 318-71) and Commentary (ACI 318R-71)*. Farmington Hills, MI: American Concrete Institute (ACI).
10. Hsu, T. C. 1984. *Torsion of Reinforced Concrete*. New York, NY: Van Nostrand Reinhold Publishers.

## Notation

$a$  = vertical distance from the bottom of a spandrel to the center of the lower tieback connection

$A_s''$  = total area of steel required on the inner web face crossing the critical diagonal crack in a direction perpendicular to the crack

$A_{sh}$  = required hanger steel

$A_{si}$  = total required area of vertical steel on inner web face

$A_{si}/s$  = total quantity of distributed vertical steel required on inner web face

$A_{sl}$  = total required area of horizontal steel on inner face to resist plate bending

$A_{sl}/s$  = distributed longitudinal steel required on inner web face for plate bending

$A_{so}$  = total distributed vertical reinforcement required on outer web face

$A_{sv}$  = total required area of steel crossing diagonal crack in vertical direction

$A_{sv2}$  = total quantity of vertical steel crossing line 2-2 on inner face

$A_v$  = area of shear reinforcement

$A_v/s$  = uniformly distributed vertical shear reinforcement

$b$  = thickness of web

$d$  = distance from extreme compression fiber to centroid of longitudinal reinforcement

$d_w$  = effective depth from outer surface of web to centroid of combined horizontal and vertical steel reinforcement of web; usually taken as web thickness less concrete cover less diameter of inner-face vertical steel bars

$e$  = eccentricity

$f_c'$  = specified concrete compressive strength

$f_{cr}$  = diagonal tensile stress due to plate bending of a slender spandrel

$f_y$  = yield strength of mild steel

$h$  = height of spandrel section

$h/b$  = aspect ratio

$H_1$  = measured lower lateral tieback reaction

$H_2$  = measured deck connection forces

$H_3$  = measured upper lateral tieback reaction

$H_{nt}$  = out-of-plane force resultants

$l_{ch}$  = length of horizontal projection of diagonal crack

$L_{twist}$  = lever arm

$M_u$  = factored bending moment

$P_u$  = factored stem load

$s$  = spacing of vertical reinforcement

$T$  = applied torque

$T_{nb}$  = nominal plate-bending resistance of web

$T_{nt}$  = nominal twist resistance of section

$T_t'$  = twisting moment at failure

$T_u$  = factored torque

$T_{ub}$  = plate-bending component of torsion

$T_{ut}$  = twisting component of torsion

$V$  = experimentally measured main spandrel end reaction

$V_a$  = experimentally applied stem reaction

$V_c$  = nominal concrete shear strength = lesser of  $V_{ci}$  or  $V_{cw}$  as given by Eq. (11-11) and (11-12) of ACI 318-08<sup>7</sup>

$V_{ci}$  = nominal shear strength provided by concrete when diagonal cracking results from combined shear and moment

$V_{cr}$  = shear force at cracking



$V_{cw}$	= nominal shear strength provided by concrete when diagonal cracking results from high principal tensile stress in web	$\Sigma V$	= sum of measured vertical reactions at failure
$V_u$	= factored shear force	$\Sigma V_a$	= sum of loads applied to the spandrel by the double-tee decks and jacks
$X$	= out-of-plane shear-stress coefficient	$\Sigma V_s$	= self-weight of the spandrel beam
$X^*$	= height of centroid	$\Sigma \mu_v$	= sum of lateral forces at the main vertical bearing due to friction
$\bar{X}$	= extreme values of stress distribution	$\Sigma \mu_{va}$	= sum of lateral forces at the ledge (or corbel) due to friction
$X_{avg}$	= average of $X^*$ and $\bar{X}$	$\phi_f$	= strength reduction factor for flexure = 0.9
$X \sqrt{f'_c}$	= effective out-of-plane shear stress	$\phi_s$	= strength reduction factor for shear = 0.75
$X_v$	= distance from outer web face to center of main vertical reaction, estimated to remain at center of the web		
$X_{va}$	= distance from outer web face to center of ledge reactions, estimated to remain at center of ledge bearing pads		
$X_{vs}$	= distance from outer web face to center of self-weight reaction, estimated to remain at center of gravity		
$Z_{H1}$	= height of lower lateral reaction		
$Z_{H2}$	= height of deck connection		
$Z_{H3}$	= height of upper lateral reaction		
$Z_{\mu v}$	= height to Teflon surface of main bearing pad		
$Z_{\mu va}$	= height to Teflon surface of ledge (or corbel) bearing pad		
$Z_t$	= height of twist axis		
$\theta$	= critical diagonal crack angle for region under consideration with respect to horizontal		
	= 45 deg for end regions		
	= 30 deg for transition regions		
	= 0 deg for flexure regions		
$\mu$	= friction coefficient		
$\Sigma H_1$	= sum of measured lower lateral reactions at failure		
$\Sigma H_2$	= sum of lateral forces at the deck connections		
$\Sigma H_3$	= sum of measured upper lateral reactions at failure		



## Appendix: Design example

### Problem statement

Determine the reinforcement required in the web of the simply supported, L-shaped spandrel beam (**Fig. A1**). The spandrel supports nine double-tee stems, each spaced 5 ft (1.5 m) apart. One stem is centered at midspan. Each stem reaction comprises a dead-load reaction of 10.74 kip (47.8 kN), a live-load reaction of 6 kip (27 kN), and a snow-load reaction of 4.5 kip (20 kN). Stem loads are centered 6 in. (150 mm) from the inside web face.  $1.2D + 1.6L + 0.5S$  is the controlling load case. The spandrel self-weight is 567 lb/ft (8.27 kN/m).

### Given information

Web thickness  $b = 8$  in. (200 mm)

Web depth  $h = 60$  in. (1500 mm)

Eccentricity  $e = 10$  in. (250 mm)

Span = 44 ft 6 in. (13.6 m)

Depth of web steel  $d_w = 6.5$  in. (165 mm)

Concrete design strength  $f'_c = 6000$  psi (40 MPa)

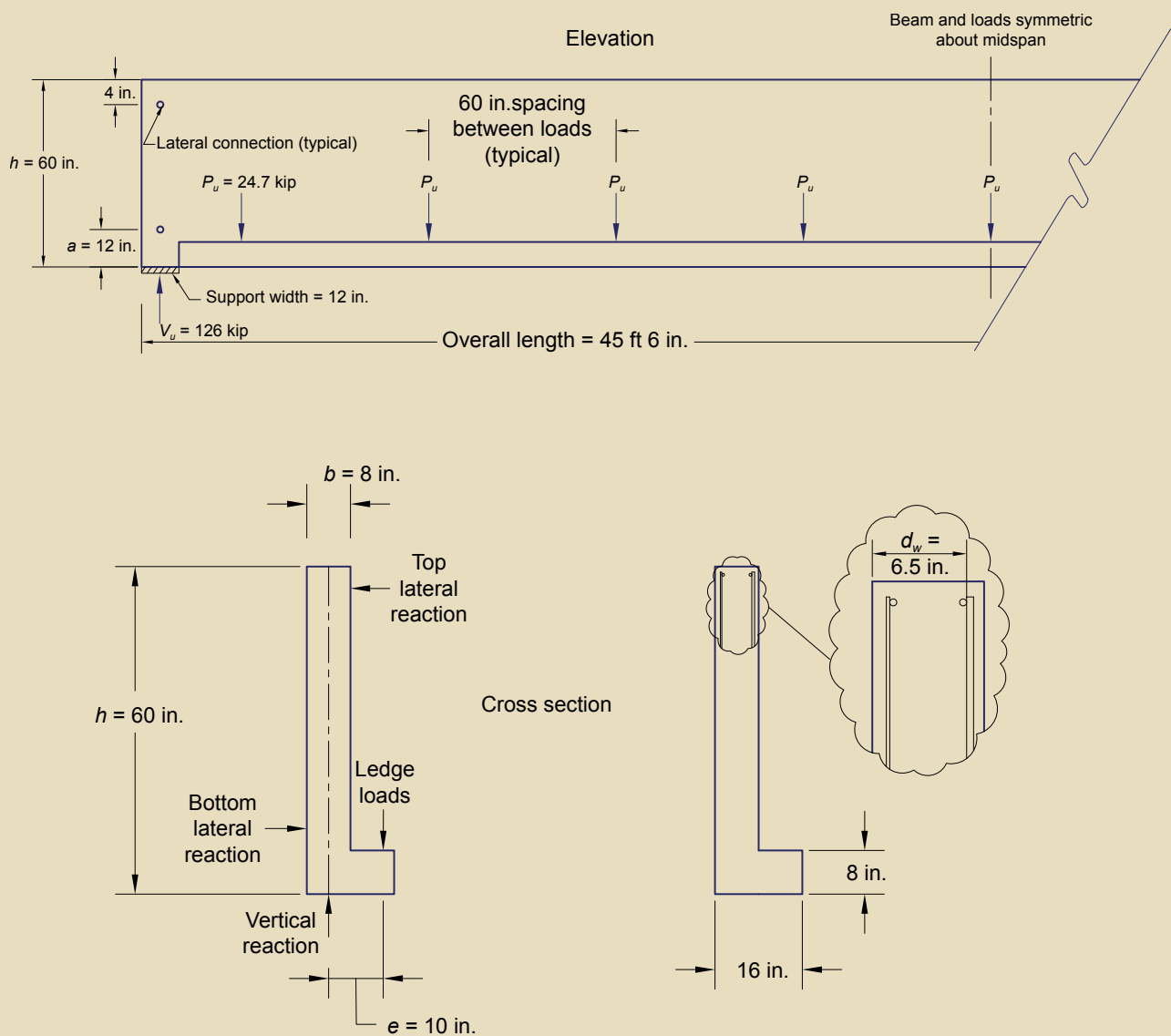


**Figure A1.** L-shaped spandrel considered in design example. Note:  $a$  = vertical distance from bottom of spandrel to center of lower tie-back connection;  $b$  = thickness of web;  $d_w$  = effective depth from outer surface of web to centroid of combined horizontal and vertical steel reinforcement of web; usually taken as web thickness less concrete cover less diameter of inner-face vertical steel bars;  $e$  = eccentricity;  $h$  = height of spandrel;  $P_u$  = factored stem load;  $V_u$  = factored shear force. 1 in. = 25.4 mm; 1 ft = 0.305 m; 1 kip = 4.448 kN.

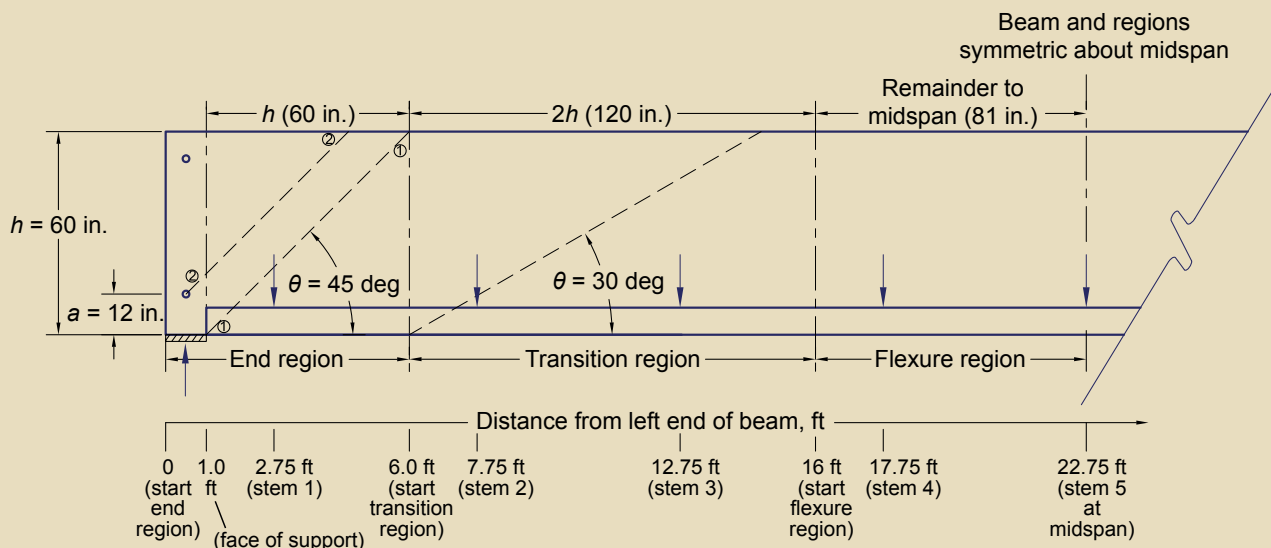


**Figure A2.** Divide spandrel beam into three regions (step 2). Note:  $a$  = vertical distance from bottom of spandrel to center of lower tie-back connection;  $h$  = height of spandrel;  $\theta$  = critical diagonal crack angle for region under consideration with respect to horizontal. 1 in. = 25.4 mm; 1 ft = 0.305 m.

Yield strength of mild steel  $f_y = 60,000$  psi (410 MPa)

Aspect ratio  $h/b = 7.5$

### Given sketches

Figure A1 and Fig. A2 provide additional information for this example.

### Solution

The beam meets the following criteria, so the design approach presented in this paper may be used:

- A simply supported precast concrete spandrel is loaded along the bottom edge of the web.
- The web is laterally restrained at two points at each end.
- Applied loads are evenly spaced along the bottom edge of the web.
- The aspect ratio of 7.5 (height divided by web thickness) is greater than or equal to 4.6.

### Step 1: Determine the loading demands

The maximum factored bending moment at midspan  $M_u = 1440$  kip-ft (1950 kN-m)

The maximum factored vertical shear at the face of the support  $V_u = 126$  kip (560 kN)

The maximum factored torque at the support  $T_u = 1113$  kip-in. (125.8 kN-m)

$$T_u = \left[ 1.2(10.74) + 1.6(6) + 0.5(4.5) \right] \left( \frac{9}{2} \right) (10)$$

$T_u = 1113$  kip-in. (125.8 kN-m)

The eccentric self-weight of the ledge is neglected.

### Step 2: Divide the slender spandrel into three regions

Figure A3 shows the divisions of the slender spandrel into three regions.

### Step 3: Verify that the cross section can sustain the twisting component of torsion

Verify that the maximum torque  $T_u$  in the end region does not exceed the twist limit for this region by considering Eq. (23).

Typically, a section is checked for the twisting component of torsion about the 1-1 crack.

$$T_u \leq \phi_s \left( 1.13 \sqrt{f'_c} d_w h^2 \right) \quad (23)$$

$$T_u \leq \frac{0.75 \left[ (1.13) \sqrt{6000} (6.5) (60)^2 \right]}{1000 \text{ lb/kip}}$$

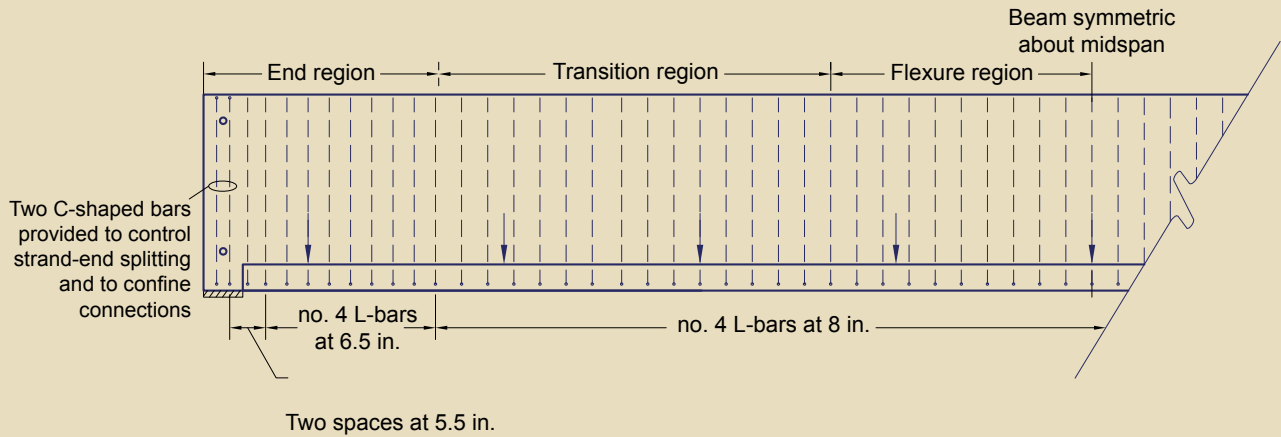


**Figure A3.** Elevation view of vertical bars provided on inner web face (step 7). Note: no. 4 = 13M; 1 in. = 25.4 mm.

$$T_u \leq 1536 \text{ kip-in. (173.5 kN-m)}$$

$T_u = 1113 \leq 1536 \text{ kip-in. (125.8 < 173.5 kN-m)}$  **The section is OK for twist**

Check that lateral connection spacing exceeds  $0.6h$ .

$$\text{Spacing} = 60 - 12 - 4 = 44 \text{ in. (1100 mm)}$$

$$44 \text{ in.}/60 \text{ in.} = 0.73$$

$$0.73h > 0.6h$$

The lateral connection spacing is sufficient; thus, a check for twist on the 2-2 crack is not required.

#### Step 4: Design the beam for flexure

The beam is designed for flexure using the techniques in section 4.2 of the *PCI Design Handbook* (not shown). Thirteen longitudinal prestressing strands are selected to provide flexural resistance.

#### Step 5: Calculate the required shear steel at all sections along the beam

The beam is designed for vertical shear using the techniques in section 4.3 of the *PCI Design Handbook* (not shown). For the vertical shear design in this step, eccentricity is ignored. The vertical shear steel required ( $A_{sv}/s$ ) is determined to be  $0.08 \text{ in.}^2/\text{ft}$  at all locations (**Table A1**).  $V_c$  is relatively high in this example; thus, minimum steel requirements govern.

#### Step 6: Calculate the vertical reinforcement required on the inner web face to resist the plate-bending component of torsion

Plate bending is considered in the end region and in the transition region. There is no need to consider plate bending in the flexure region. The vertical steel required to resist plate bending is calculated using the maximum  $T_u$  from each region.

For the end region (maximum  $T_u$  in this region is 1113 kip-in. [125.8 kN-m]):

$$A_{sv}/s \geq \frac{T_u}{2\phi_f f_y d_w h} \quad (24)$$

$$A_{sv}/s \geq \frac{1,113,000}{2(0.9)(60,000)(6.5)(60)}$$

$$A_{sv}/s \geq 0.0264 \text{ in.}^2/\text{in. (670 mm}^2/\text{m)}$$

$$A_{sv}/s \geq 0.317 \text{ in.}^2/\text{ft (670 mm}^2/\text{m)}$$

For the transition region (maximum  $T_u$  in this region is 866 kip-in. [97.8 kN-m]):

$$A_{sv}/s \geq \frac{T_u}{2.3\phi_f f_y d_w h} \quad (25)$$

**Table A1.** Vertical shear steel requirement

Distance from left end of beam, ft	1	2.75	6.0	7.75	12.75	16.0	17.75	22.75
Shear steel required, in. <sup>2</sup> /ft	0.08	0.08	0.08	0.08	0.08	0.08	0.08	0.08

Note: 1 in. = 25.4 mm; 1 ft = 0.305 m.



**Table A2.** Shear and torsion steel requirements, inner web face

Beam region	End			Transition			Flexure	
Distance from left end of beam, ft	1	2.75	6.0	7.75	12.75	16.0	17.75	22.75
Shear steel $A_v/s$ , in. <sup>2</sup> /ft	0.08	0.08	0.08	0.08	0.08	0.08	0.08	0.08
$1/2(A_v/s)$ , in. <sup>2</sup> /ft	0.04	0.04	0.04	0.04	0.04	0.04	0.04	0.04
$A_{sv}/s$ , in. <sup>2</sup> /ft	0.317	0.317	0.317	0.215	0.215	0.215	0	0
Steel required on inner web face for shear and torsion, in. <sup>2</sup> /ft*	0.357	0.357	0.357	0.255	0.255	0.255	0.04	0.04

\*Other inner-face steel requirements, such as hanger steel, may still control design. Using section 4.5 of *PCI Design Handbook*, required hanger steel  $A_{sh}$  is 0.222 in.<sup>2</sup>/ft (470 mm<sup>2</sup>/m) (not shown). In addition, hanger steel design dictates that hanger bar spacing not exceed ledge depth of 8 in. (200 mm). Hanger steel requirement is not additive. Thus, designer should choose larger of hanger steel requirement or shear/torsion steel requirement at given location.

Note:  $A_{sv}$  = area of vertical plate-bending reinforcement;  $A_v$  = area of shear reinforcement;  $s$  = spacing of vertical reinforcement. 1 in. = 25.4 mm; 1 ft = 0.305 m.

$$A_{sv}/s \geq \frac{886,000}{2.3(0.9)(60,000)(6.5)(60)}$$

$$A_{sv}/s \geq 0.0179 \text{ in.}^2/\text{in.} \quad (460 \text{ mm}^2/\text{m})$$

$$A_{sv}/s \geq 0.215 \text{ in.}^2/\text{ft} \quad (460 \text{ mm}^2/\text{m})$$

### Step 7: Proportion the vertical steel on the inner web face

Vertical steel is provided for shear and torsion on the inner web face (ledge or corbel side) to satisfy Eq. (26) at all locations:

$$A_{sv}/s \geq \left( A_{sv} + \frac{1}{2}A_v \right) / s \quad (26)$$

**Table A2** lists the values of the shear and torsion steel requirements on the inner web face.

Vertical L-shaped bars are spaced on the inner web face (**Fig. A4**) to satisfy the shear/torsion and hanger steel requirements.

The no. 4 (13M) reinforcing bars spaced at 6.5 in. (165 mm) satisfy the 0.357 in.<sup>2</sup>/ft (750 mm<sup>2</sup>/m) required in the end region. The no. 4 reinforcing bars spaced at the hanger steel limit of 8 in. (200 mm) satisfy the 0.255 in.<sup>2</sup>/ft (540 mm<sup>2</sup>/m) required in the transition zone and also the 0.222 in.<sup>2</sup>/ft (470 mm<sup>2</sup>/m) required at all locations for hanger steel. Two C-shaped bars are provided at each end of the beam to confine the connection zone and control longitudinal splitting at the ends of the prestressing strands. The remaining bars are L-shaped bars.

### Step 8: Check the plate-bending capacity about line 2-2 in the end region

Plate bending about line 2-2 may be more critical than plate bending about line 1-1 in the end region (**Fig. A1** and **A2**). Whether line 2-2 is critical for plate bending depends on the location of the lateral tieback reactions and on the quantity of vertical shear steel  $A_v$ . After proportioning the vertical steel in step 7, verify that the total quantity of vertical steel crossing line 2-2 on the inner face exceeds Eq. (27).

$$A_{sv2} \geq \frac{T_u}{\phi_f 2f_y d_w} \quad (27)$$

$$A_{sv2} \geq \frac{1,113,000}{(0.9)(2)(60,000)(6.5)}$$

$$A_{sv2} \geq 1.59 \text{ in.}^2 \quad (1030 \text{ mm}^2)$$

Eight vertical no. 4 (13M) reinforcing bars cross the 2-2

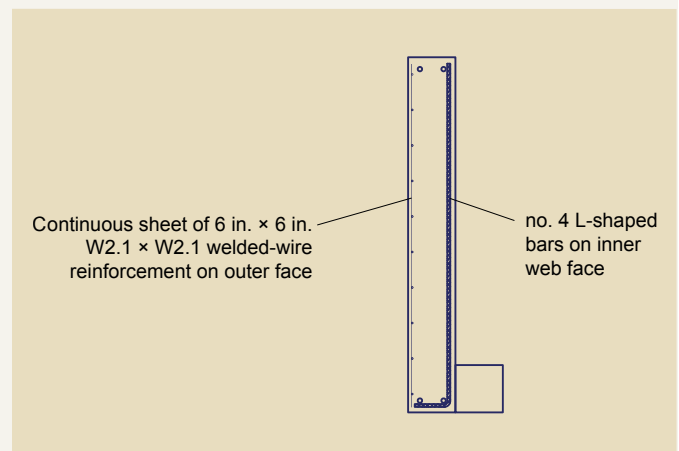


**Figure A4.** Profile view of web steel (step 9). Note: no. 4 = 13M; 1 in. = 25.4 mm.

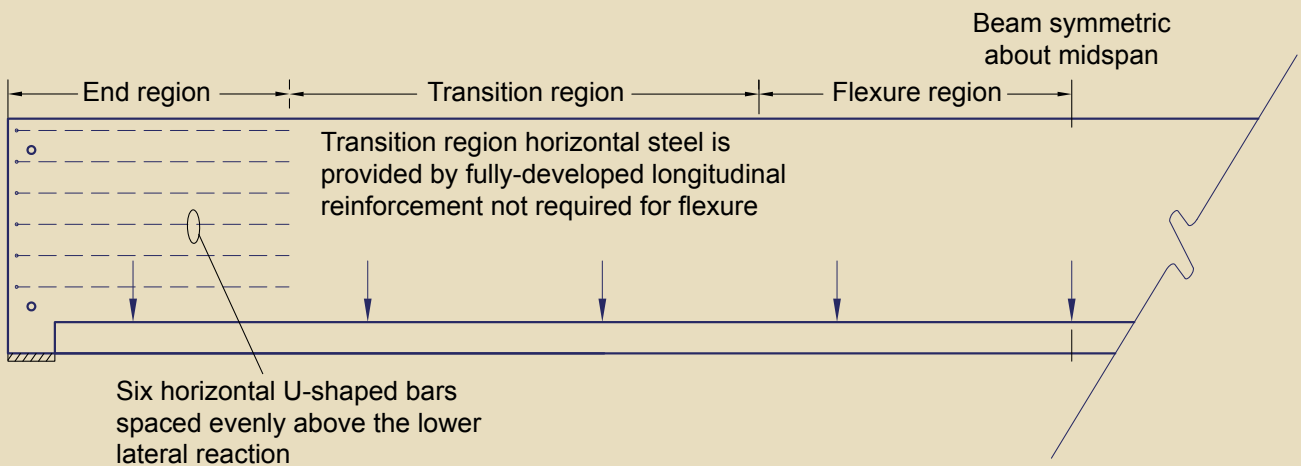


**Figure A5.** Horizontal U-shaped bars provided in end region (step 11).

crack plane, providing 1.60 in.<sup>2</sup> (1030 mm<sup>2</sup>) of steel and satisfying the  $A_{sv2}$  requirement.

### Step 9: Proportion the vertical steel on the outer web face

Vertical steel is provided on the outer web face to satisfy Eq. (28) at all locations.

$$A_{sv} \geq \frac{1}{2} A_v \quad (28)$$

$A_v$  was calculated in step 5. Thus, the vertical steel required on the outer face  $A_{sv}$  for shear and torsion is 0.04 in.<sup>2</sup>/ft (85 mm<sup>2</sup>/m) at all locations. A continuous sheet of 6 in. × 6 in. (150 mm × 150 mm), W2.1 × W2.1 welded-wire reinforcement will satisfy this requirement (**Fig. A5**).

### Step 10: Calculate the longitudinal reinforcement required to resist the plate-bending component of torsion

The total quantity of longitudinal steel required to resist plate bending is determined.

For the end region (maximum  $T_u$  in this region is 1113 kip-in. [125.8 kN-m]):

$$A_{sl} \geq \frac{T_u}{2\phi_f f_y d_w} \quad (29)$$

$$A_{sl} \geq \frac{1,113,000}{(2)(0.9)(60,000)(6.5)}$$

$$A_{sl} \geq 1.59 \text{ in.}^2 \text{ (1030 mm}^2\text{)}$$

For the transition region (maximum  $T_u$  in this region is 866 kip-in. [97.8 kN-m]):

$$A_{sl} \geq \frac{T_u}{2.3\phi_f f_y d_w} \quad (30)$$

$$A_{sl} \geq \frac{886,000}{(2.3)(0.9)(60,000)(6.5)}$$

$$A_{sl} \geq 1.07 \text{ in.}^2 \text{ (690 mm}^2\text{)}$$

### Step 11: Proportion the longitudinal web steel for plate bending

Six no. 5 (16M), horizontal U-bars provide the required longitudinal steel on each face in the end region. All bars are located above the lower lateral reaction.

Sufficient fully developed excess flexural reinforcement may be used in the transition zone to satisfy the longitudinal steel requirement. In this example, prestressing strands not required for flexural reinforcement are used to meet the longitudinal plate-bending steel requirement in the transition zone. The longitudinal steel required in this zone  $A_{sl}$  (as previously calculated assuming 60 ksi [420 MPa]) can be reduced proportionally according to the increase in steel strength (from 60 ksi to 270 ksi [420 MPa to 1860 MPa]). Thus, 0.24 in.<sup>2</sup> (150 mm<sup>2</sup>) of 270 ksi (1860 MPa) prestressing steel would satisfy the  $A_{sl}$  requirement in the transition zone for this example.

### Step 12: Detail the beam

Recommendations in the *PCI Design Handbook* regarding ledge design, connection detailing, hanger steel, impact steel, and reinforcement for other possible localized failure



modes are to be considered. In addition, it is recommended that continuous bars or strands be placed in the longitudinal direction at all four corners of the web to control the possible cracking from lateral bending away from the ends.

### Step 13: Check service-level cracking

If desired, the load at which diagonal cracking in the end region is first likely to appear may be conservatively estimated according to Eq. (31). In many cases, beams will be cracked at service load, regardless of end-region reinforcement. First cracking load is independent of web reinforcement configuration (that is, open or closed stirrups). The effects of prestressing are ignored in Eq. (31) because some of the prestressing strands are not fully developed across the potential crack.

$$V_{cr} = \left[ \frac{4\sqrt{f'_c}}{(1 + 2e/b)} \right] bh \quad (31)$$

where

$V_{cr}$  = shear force at cracking

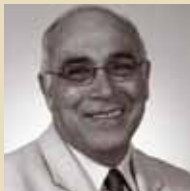
## About the authors



Gregory Lucier is a laboratory manager for North Carolina State University in Raleigh, N.C.



Catrina Walter is an engineer for BergerABAM in Federal Way, Wash.



Sami Rizkalla is a distinguished professor for North Carolina State University in Raleigh.



Paul Zia is a distinguished university professor emeritus for North Carolina State University in Raleigh.



Gary Klein is executive vice president and senior principal for Wiss, Janney, Elstner Associates Inc. in Northbrook, Ill.

## Synopsis

This paper summarizes the results of an analytical research program undertaken to develop a rational design procedure for normalweight precast concrete slender spandrel beams. The analytical and rational models use test results and research findings of an extensive experimental program presented in the companion paper “Development of a Rational Design Methodology for Precast Concrete Slender Spandrel Beams: Part 1, Experimental Results,” which appeared in the Spring 2011 issue of *PCI Journal*. The overall research effort demonstrated the validity of using open web reinforcement in precast concrete slender spandrel beams and proposed a simplified procedure for design. The webs of such slender spandrels, particularly in their end regions, are often heavily congested with reinforcing cages when designed with current procedures. The experimental and analytical results demonstrate that open web reinforcement designed according to the proposed procedure is safe and effective and provides an efficient alternative to traditional closed stirrups for precast concrete slender spandrel beams..

## Keywords

Open reinforcement, slender spandrel beam, torsion, twist.

## Review policy

This paper was reviewed in accordance with the Precast/Prestressed Concrete Institute’s peer-review process.

## Reader comments

Please address any reader comments to [journal@pci.org](mailto:journal@pci.org) or Precast/Prestressed Concrete Institute, c/o *PCI Journal*, 200 W. Adams St., Suite 2100, Chicago, IL 60606. 